

Probing non-equilibrium steady states of the Klein-Gordon field with Unruh-DeWitt detectors

Albert Georg Passegger^{*1,2}, Rainer Verch^{†1,3}

¹Institut für Theoretische Physik, Universität Leipzig, Leipzig, Germany

²Max Planck Institute for Mathematics in the Sciences, Leipzig, Germany

³CY Advanced Studies, CY Cergy Paris Université, Neuville-sur-Oise, France

Abstract

We calculate the transition rate of an Unruh-DeWitt detector coupled to a non-equilibrium steady state (NESS) of a free massless scalar field on four-dimensional Minkowski spacetime. The NESS arises from bringing two semi-infinite heat baths into thermal contact along a hypersurface. The detector couples linearly to the field by a monopole interaction, and it moves inertially along the axis of the NESS heat flow. We contrast the resulting transition rates with the case of a detector that is coupled to an inertial thermal equilibrium state. The results illustrate that the monopole does not properly couple to the heat flow, resulting in the detector to merely register kinematical effects. Hence dynamical features of the NESS are hidden from this detector model.

1. Introduction

Non-equilibrium steady states (NESS) [Rue00, JP02a] describe configurations of systems that are out of thermal equilibrium, but still are stationary under the time evolution. NESS of quantum systems have been considered in various models and contexts, and we refer to [Rue01, Rue02, JP02b, Oga04, MMS07a, MMS07b, Abo07] for a limited selection of works. A conceptually simple class of NESS may arise from bringing two semi-infinite heat baths (thermal reservoirs) at different temperatures into thermal contact, a model that is also referred to as a “quench” [DLSB15] (see also [BD12, BD15, HD15, BDLS15, HL18] in the context of conformal field theory, [SL77, Tas01, AP03] for similar models, and further literature referenced in these works). Under the energy exchange between the baths, such a system can settle at asymptotically late times in a stationary configuration with a heat (energy) flow in an intermediate region from the higher to the lower temperature heat bath. A NESS of this kind

^{*}e-mail: albert_georg.passegger@uni-leipzig.de

[†]e-mail: rainer.verch@uni-leipzig.de

has been constructed in [DLSB15, HV18] for initial heat baths described by KMS states of scalar (Klein-Gordon) quantum fields on Minkowski spacetime coupled along a hypersurface.

In the present paper we probe the NESS of [HV18] for a free massless scalar field on four-dimensional Minkowski spacetime using a two-level Unruh-DeWitt monopole detector [Unr76, DeW79, BD82, UW84, Tak86]. We derive the asymptotic transition rate (number of transitions per unit proper time) of the detector in first-order time-dependent perturbation theory and contrast it with the transition rates of inertially moving detectors coupled to inertial thermal equilibrium states characterized by the KMS (Kubo-Martin-Schwinger) condition [Kub57, MS59, HHW67, Haa96, BR97].

The topic is motivated by our recent work [PV25], where we discussed the late time behavior of a coupled system comprised of an Unruh-DeWitt detector that moves with constant velocity relative to an inertial KMS state of a massless scalar field. The results of [PV25] indicate that the non-thermalization of the system relative to the inertial rest frame of the detector can be traced back to the disjointness of KMS states in different inertial frames (i.e. two distinct KMS states in different inertial frames cannot be generated from one another via local operations). That inertially moving detectors in a heat bath will not approach thermal equilibrium is supported by the transition rate calculated in [CM95b], which shows that the detector is affected by the motion-induced Doppler shift of the bath's thermal radiation relative to the detector's rest frame (see also [CM95a, LM96, LM04]). The form of the asymptotic density matrix of the detector calculated in [PA20], and the impossibility for a state to satisfy the KMS condition relative to two different inertial frames [Sew08, Sew09], further corroborate this picture.

Based on these observations one might think that the anisotropy and apparent heat flow of a thermal reservoir from the perspective of the detector's rest frame is modeled by a NESS. However, it is important to note that the NESS we consider here does not satisfy the KMS condition with respect to any inertial reference frame (except for the two-dimensional massless scalar field [DLSB15]; see also [HV18, Sec. 3.2]). Still, depending on the model, the response of a detector in terms of its transition rate could be comparable for a moving detector in a heat bath and in a NESS. We thus opt for an investigation of NESS in such a detector-dependent setup, focusing on the question of what a monopole Unruh-DeWitt detector can “see” from the NESS in its transition rate.

In Section 2 the basic setup is introduced. We review the transition rate of an Unruh-DeWitt detector coupled to a massless Klein-Gordon field and briefly introduce the NESS of the field according to [HV18]. In Section 3 we calculate and discuss the transition rates of a detector at rest and moving inertially along the longitudinal axis of the NESS as well as relative to a KMS heat bath under a monopole interaction. Some aspects of the detector's effective detailed balance temperatures in these cases are discussed in Section 4, and we define the comoving frame of the NESS in Section 5. Our work represents a first step in the study of

NESS from the perspective of detector systems, a topic which, to the best of our knowledge, has not received much attention yet. Section 6 summarizes our findings and outlines open problems that could be picked up in the future. Additional material (consisting of mostly previously established results) is collected in four appendices, one of them (Appendix A) providing a detailed derivation of the transition rate for a detector moving with constant velocity through a scalar field heat bath, which has been presented in [CM95a, CM95b].

Conventions and remarks We use the “mostly minus” metric signature $(+, -, -, -)$, and physical units where the vacuum speed of light, reduced Planck constant, and Boltzmann constant are set to 1. The plots were generated using the L^AT_EX package PGFPlots (<https://ctan.org/pkg/pgfplots>). The surface (mesh) plots are colored (with interpolation shading) as a visual aid according to the value of the function (z -axis; “lower = blue”, “higher = yellow”).

2. Preliminaries and setup

2.1. The detector-field system

A two-level Unruh-DeWitt detector [Unr76, DeW79, BD82, UW84, Tak86] (henceforth simply called “detector”) is a quantum system with Hilbert space \mathbb{C}^2 and Hamiltonian $H_D = \text{diag}(E, 0)$ with respect to orthonormal basis vectors $|E\rangle$ and $|0\rangle$ of eigenvalues $E \in \mathbb{R} \setminus \{0\}$ and 0, respectively, where E represents the energy gap of the system. Depending on the sign of E the vector $|0\rangle$ represents the ground (for $E > 0$) or excited state (for $E < 0$), and vice versa for $|E\rangle$. A transition from $|0\rangle$ to $|E\rangle$ is thus interpreted either as an excitation ($E > 0$) or a decay (de-excitation, $E < 0$) of the detector.

The quantum field under consideration is a free massless real scalar (Klein-Gordon) field on four-dimensional Minkowski spacetime \mathbb{M} , and we essentially follow the setup described in [HV18]. Points in Minkowski spacetime $\mathbb{M} \cong \mathbb{R}^4$ relative to coordinate axes of an inertial reference frame will be denoted by $x \equiv (x^0, \underline{x}) \equiv (x^0, x^1, x^2, x^3)$. The field equation is given by $(\partial_0^2 - \sum_{j=1}^3 \partial_j^2)\phi = 0$, where $\partial_\mu := \frac{\partial}{\partial x^\mu}$ for $\mu \in \{0, 1, 2, 3\}$. The quantum field theory can be described by a topological $*$ -algebra \mathcal{A} generated by formal symbols $\{\mathbb{1}, \phi(f) : f \in C_c^\infty(\mathbb{R}^4)\}$ subject to the usual relations implementing linearity, canonical commutation relations, and the field equation; see, e.g., [KM15, FR20] for details. The generators $\phi(f)$ are interpreted as “smeared field operators”, which motivates the common integral kernel notation $\phi(f) = \int_{\mathbb{M}} \phi(x)f(x) dx$. On \mathcal{A} the time evolution along the time direction determined by the x^0 -axis is given by the one-parameter $*$ -automorphism group $\alpha = \{\alpha_t\}_{t \in \mathbb{R}}$ with

$$\alpha_t(\phi(x^0, \underline{x})) = \phi(x^0 + t, \underline{x}). \quad (2.1)$$

Smearing with a compactly supported smooth function $f \in C_c^\infty(\mathbb{R}^4)$ this means that $\alpha_t(\phi(f)) = \phi(f \circ T_{-t})$ for the time translation isometries $T_t : (x^0, \underline{x}) \mapsto (x^0 + t, \underline{x})$ on \mathbb{M} .

Let ω be a state (i.e. a positive, normalized, linear functional) on \mathcal{A} . There exists a $*$ -representation π_ω of \mathcal{A} by linear operators on a dense subspace \mathcal{D}_ω of a Hilbert space \mathcal{H}_ω and a normalized vector $\Omega_\omega \in \mathcal{D}_\omega$, such that $\omega(A) = \langle \Omega_\omega, \pi_\omega(A)\Omega_\omega \rangle$ for all $A \in \mathcal{A}$ and $\pi_\omega(\mathcal{A})\Omega_\omega = \mathcal{D}_\omega$. The data $(\pi_\omega, \mathcal{H}_\omega, \mathcal{D}_\omega, \Omega_\omega)$ is called the GNS representation of ω and is unique up to unitary equivalence (see, e.g., [KM15, FR20]). If ω is α -invariant, i.e. $\omega \circ \alpha_t = \omega$ for all $t \in \mathbb{R}$, then the time translations are generated by a Hamiltonian H_ω on the GNS space \mathcal{H}_ω , that is, $\frac{d}{dt}\pi_\omega(\alpha_t(A))|_{t=0} = i[H_\omega, \pi_\omega(A)]$ for $A \in \mathcal{A}$. The domain of H_ω contains the dense subspace $\pi_\omega(\mathcal{A})\Omega_\omega$, which is invariant under H_ω . The quantum field is represented by an operator-valued distribution $f \mapsto \Phi(f)$ with unbounded operators $\Phi(f) := \pi_\omega(\phi(f)) = \int_{\mathbb{M}} \Phi(x)f(x) dx$ as quadratic forms on \mathcal{D}_ω , which is used to define $\Phi(x)$ for $x \in \mathbb{M}$. In the GNS representation of the Minkowski vacuum, which is a ground state with respect to any inertial time translation, we have $\Phi(x) = (2\pi)^{-3/2} \int_{\mathbb{R}^3} (2\|\underline{p}\|)^{-1/2} (e^{ip \cdot x} a^*(\underline{p}) + e^{-ip \cdot x} a(\underline{p})) d^3 \underline{p}$ for $p \cdot x = \|\underline{p}\|x^0 - \underline{p} \cdot \underline{x}$ and annihilation and creation operators a, a^* on the bosonic Fock space over the one-particle space $L^2(\mathbb{R}^3, d^3 \underline{x})$, obeying the commutation relations $[a(\underline{p}), a^*(\underline{p}')] = \delta(\underline{p} - \underline{p}')$. For details on these topics we refer to [KM15, FR20]).

An important class of states is given by quasi-free (also called ‘‘Gaussian’’) Hadamard states. They are completely determined by their two-point function, which is of Hadamard form (i.e., the short-distance behavior approximates the vacuum state), and their odd n -point functions vanish [KW91, Rad96, KM15]. The α -invariant quasi-free Hadamard states considered in this work are the NESS introduced in Section 2.3 [HV18], and the KMS states ω_β on \mathcal{A} for $\beta > 0$ with respect to α (which satisfy the Hadamard condition by [SV00]), representing inertial thermal equilibrium states of the field [HHW67, Haa96, BR97] (see also [HV18, Sec. 2.1]).

2.2. Coupling, transition rate, and two-point functions

Let ω be a quasi-free Hadamard state of the field with GNS representation $(\pi_\omega, \mathcal{H}_\omega, \mathcal{D}_\omega, \Omega_\omega)$, and $\mathbf{x} : \mathbb{R} \rightarrow \mathbb{M}$, $\tau \mapsto \mathbf{x}(\tau)$ a smooth timelike curve representing the worldline of the detector parametrized in proper time $\tau \in \mathbb{R}$. The free time evolution of the combined detector-field system is assumed to be generated by a Hamiltonian $H_D \otimes \mathbb{1} + \mathbb{1} \otimes H_\omega$ on $\mathbb{C}^2 \otimes \mathcal{H}_\omega$ with respect to proper time. We let the detector-field system evolve under a (point-like) monopole interaction linear in the field, implemented in the interaction picture by adding a Hamiltonian of the form (see, e.g., [BD82, LS08, FJL16])

$$\lambda \chi(\tau) \mu(\tau) \otimes \Phi(\mathbf{x}(\tau)). \quad (2.2)$$

Here, $\lambda \in \mathbb{R}$ is the coupling parameter, and χ is a real-valued, non-negative (but not identically vanishing), smooth function, called the switching function, whose support determines the times during which the coupling between detector and field is active. The operator $\mu(\tau) =$

$e^{iH_D\tau}\mu(0)e^{-iH_D\tau}$ is the monopole moment operator of the detector at time τ for some self-adjoint bounded operator $\mu(0)$ on \mathbb{C}^2 such that $|\langle E|\mu(0)|0\rangle| \neq 0$.

Assume that before the interaction the detector is prepared in the state represented by $|0\rangle$, and the field in the state ω . The probability for the detector to be found in the state represented by $|E\rangle$ (and the field in any state) after the interaction is $\lambda^2|\langle E|\mu(0)|0\rangle|^2\mathcal{F}_{\omega,\chi}(E)$ in first-order perturbation theory in λ [Unr76, DeW79, BD82, LS08, FJL16], where $\mathcal{F}_{\omega,\chi}$ is the *response function* defined by (for suitable χ , e.g. smooth compactly supported or Schwartz function)

$$\mathcal{F}_{\omega,\chi}(E) := \int_{\mathbb{R}} \int_{\mathbb{R}} e^{-iE(\tau-\tau')} \chi(\tau)\chi(\tau') W_{\omega}(\mathbf{x}(\tau), \mathbf{x}(\tau')) \, d\tau \, d\tau'$$

for the two-point (positive-frequency Wightman) correlation function W_{ω} in the state ω :

$$W_{\omega}(x, y) := \omega(\phi(x)\phi(y)) \equiv \langle \Omega_{\omega}, \Phi(x)\Phi(y)\Omega_{\omega} \rangle, \quad x, y \in \mathbb{M} \quad (2.3)$$

Apart from prescribed internal quantities of the detector system, the transition probability is therefore determined by the response function. Since $W_{\omega}(x, y) = \overline{W_{\omega}(y, x)}$, the response function is real-valued. Due to the bidistributional nature of the two-point function, closed form expressions of $W_{\omega}(x, y)$ usually need to be regularized by an $i\epsilon$ -prescription. The Hadamard property of ω entails a good control over the singular part of W_{ω} [KW91, Rad96, KM15]. As discussed in [LS08] one can specify functions $W_{\omega}^{(\epsilon)}$, $\epsilon > 0$, with the property that smearing them with test functions and taking $\epsilon \rightarrow 0_+$ results in W_{ω} ; accordingly, the integration in the definition of the response function is understood as $\lim_{\epsilon \rightarrow 0_+} \int_{\mathbb{R}} \int_{\mathbb{R}} e^{-iE(\tau-\tau')} \chi(\tau)\chi(\tau') W_{\omega}^{(\epsilon)}(\mathbf{x}(\tau), \mathbf{x}(\tau')) \, d\tau \, d\tau'$.

For the worldlines $\tau \mapsto \mathbf{x}(\tau)$ and states ω we consider in this work, the pullback of the two-point function along \mathbf{x} that appears in the response function only depends on the proper time difference between two points on the worldline, i.e. $W_{\omega}(\mathbf{x}(\tau), \mathbf{x}(\tau')) = W_{\omega}(\mathbf{x}(\tau - \tau'), \mathbf{x}(0))$ for $\tau, \tau' \in \mathbb{R}$. Let us define the distribution w_{ω} by

$$w_{\omega}(s) := W_{\omega}(\mathbf{x}(s), \mathbf{x}(0)) \quad \text{for } s \in \mathbb{R}.$$

In the limit of infinitely long interaction time, the number of detector transitions per unit proper time, the so-called transition rate, is given by the (distributional) Fourier transform of w_{ω} (see, e.g., [BD82, Sch04, LS08, FJL16, BPPL24]). Omitting the technical details one can see this as follows (see [FJL16], and the appendix of [BPPL24] for a general derivation that also discusses the various conventions appearing in the literature): Take a switching function of the form $\chi_{\theta}(\tau) = \chi(\tau/\theta)$ for some non-negative smooth function χ with $\chi(0) = 1$ and characteristic time scale given by the parameter $\theta > 0$ (this is referred to as ‘‘adiabatic scaling’’ in [FJL16]). For example, one can consider a Gaussian profile $\chi_{\theta}(\tau) = e^{-\frac{\pi\tau^2}{2\theta^2}}$, which

converges pointwise to the constant 1 as $\theta \rightarrow \infty$ (eternal constant coupling, no switching). The corresponding response function then becomes (after setting $\zeta := \tau + \tau'$, $s := \tau - \tau'$)

$$\mathcal{F}_{\omega, \chi_\theta}(E) = \frac{1}{2} \int_{\mathbb{R}} \int_{\mathbb{R}} e^{-\frac{\pi(\zeta^2 + s^2)}{4\theta^2}} e^{-iEs} w_\omega(s) \, d\zeta \, ds = \theta \int_{\mathbb{R}} e^{-iEs} e^{-\frac{\pi s^2}{4\theta^2}} w_\omega(s) \, ds.$$

The limit

$$\mathcal{R}_\omega(E) := \lim_{\theta \rightarrow \infty} \frac{1}{\theta} \mathcal{F}_{\omega, \chi_\theta}(E) = \int_{\mathbb{R}} e^{-iEs} w_\omega(s) \, ds \quad (2.4)$$

represents the *transition rate* of the detector (see [BD82, Sch04, LS08, FJL16, BPPL24]). We will exclusively focus on transition rates of detectors in the stated sense, i.e., for infinitely long interaction and sufficiently small (constant) coupling parameter conforming to first-order perturbation theory. A formula for the (in general time-dependent) transition rate at some finite time during the interaction, which takes properties of the switching function into account and applies to possibly non-stationary detector worldlines, has been given in [Sch04] and addressed in [LS08] for theories on curved spacetimes (see also [LS06, Sat07] for related discussions).

It will be useful to exploit the Hadamard property of the initial field state ω to split the transition rate into a regular and a distributional part (as has been done in, e.g., [BEG⁺20, BPPL24]). We define

$$\widetilde{W}_\omega := W_\omega - W_{\text{vac}}, \quad \widetilde{w}_\omega := \widetilde{W}_\omega(\mathbf{x}(\cdot), \mathbf{x}(0)),$$

where the two-point function of the Minkowski vacuum state (the ground state of the massless scalar field with respect to inertial time evolution) is given by

$$W_{\text{vac}}(x, y) = \frac{1}{(2\pi)^3} \int_{\mathbb{R}^3} \frac{1}{2\|\underline{p}\|} e^{-i\|\underline{p}\|(x^0 - y^0)} e^{i\underline{p} \cdot (\underline{x} - \underline{y})} \, d^3\underline{p} \quad (2.5)$$

in the sense of bidistributions (see, e.g., [FR20]). By the Hadamard property, \widetilde{W}_ω is a smooth function on $\mathbb{M} \times \mathbb{M}$ (see [KM15] and references therein).

A common expression for the vacuum two-point function along a worldline \mathbf{x} in terms of a formal, regularized integral kernel would be the $i\epsilon$ -prescription $W_{\text{vac}}(\mathbf{x}(\tau), \mathbf{x}(\tau')) = -(4\pi^2)^{-1} \lim_{\epsilon \rightarrow 0^+} ((x^0(\tau) - x^0(\tau') - i\epsilon)^2 - \|\underline{x}(\tau) - \underline{x}(\tau')\|^2)^{-1}$ (see [BD82, Eq. (3.59)]), in which it is implied that one has to integrate against test functions before taking the limit $\epsilon \rightarrow 0$ from above. An alternative, manifestly Lorentz-invariant regularization is [Sch04]

$$W_{\text{vac}}(\mathbf{x}(\tau), \mathbf{x}(\tau')) = -\frac{1}{4\pi^2} \lim_{\epsilon \rightarrow 0^+} \frac{1}{(\mathbf{x}(\tau) - \mathbf{x}(\tau') - i\epsilon(\dot{\mathbf{x}}(\tau) + \dot{\mathbf{x}}(\tau')))^2} \quad (2.6)$$

for the four-velocity \dot{x} (note that the global minus sign does not appear in [Sch04] due to the inverted choice of metric signature).

For the quasi-free β -KMS state ω_β with respect to the inertial time evolution α (Eq. (2.1)), the two-point function $W_\beta := W_{\omega_\beta}$ is given by

$$W_\beta(x, y) = \frac{1}{(2\pi)^3} \int_{\mathbb{R}^3} \frac{1}{2\|\underline{p}\|} \left(\frac{e^{i\|\underline{p}\|(x^0-y^0)} e^{-i\underline{p}\cdot(x-y)}}{e^{\beta\|\underline{p}\|} - 1} - \frac{e^{-i\|\underline{p}\|(x^0-y^0)} e^{i\underline{p}\cdot(x-y)}}{e^{-\beta\|\underline{p}\|} - 1} \right) d^3\underline{p} \quad (2.7)$$

in the sense of bidistributions (see, e.g., [FR20], and Appendix A for an equivalent representation). The vacuum two-point function in Eq. (2.5) is recovered in the limit $\beta \rightarrow \infty$.

2.3. NESS

Quasi-free NESS for linear and interacting Klein-Gordon models have been constructed in [HV18], generalizing previous results due to [DLSB15]. A discussion that covers the technical details and physical interpretation may be found in [HV18]. Here, we only give a rough description in the employed setup.

Let $\beta_L, \beta_R > 0$ be the inverse temperatures of two semi-infinite heat baths of the quantum field for $x^1 < 0$ (“left”) and $x^1 > 0$ (“right”), respectively, with respect to the time evolution α along the x^0 -axis (Eq. (2.1)). We assume these heat baths to be in contact with each other in a neighborhood of the hypersurface $\{x \in \mathbb{M} : x^1 = 0\}$, with a smoothed-out transition region $\{x \in \mathbb{M} : |x^1| < \varepsilon\}$ for some $\varepsilon > 0$. Together with an intermediate β' -KMS state on the transition region for some $\beta' \geq \beta_L, \beta_R$, the β_L - and β_R -KMS states of the heat baths are glued together by a construction using partitions of unity, which is presented in detail in [HV18, Sec. 2.2]. This results in a quasi-free Hadamard state ω_G by [HV18, Thm. 3.1]. (For simplicity, the chemical potentials of the initial semi-infinite heat baths and of the transition region between them are set to 0, so our situation falls into the third case of [HV18, (19)].) The state ω_G is a β_L - and β_R -KMS state when restricted to the Cauchy developments of $\{x \in \mathbb{M} : x^0 = 0, x^1 < -\varepsilon\}$ and $\{x \in \mathbb{M} : x^0 = 0, x^1 > \varepsilon\}$, respectively. More concretely, if $W_R := \{x \in \mathbb{M} : |x^0| < x^1\}$ is the right wedge and \mathbf{e}_1 is the spacelike unit vector along the x^1 -axis, then ω_G restricts to a β_L -KMS state on the local observable algebra $\mathcal{A}(-W_R - \varepsilon\mathbf{e}_1)$ and to a β_R -KMS state on $\mathcal{A}(W_R + \varepsilon\mathbf{e}_1)$, with respect to time evolution α . By [HV18, Thm. 3.2 (1)] the glued initial state evolves into an α -invariant, quasi-free NESS [Rue00, JP02a]

$$\omega_N = \lim_{t \rightarrow \infty} \omega_G \circ \alpha_t$$

on \mathcal{A} , completely determined by the two-point function $W_N := W_{\omega_N}$ (Eq. (2.3)) given by

$$W_N(x, y) = \frac{1}{(2\pi)^3} \int_{\mathbb{R}^3} \frac{1}{2\|\underline{p}\|} e^{i\underline{p}\cdot(x-y)} \left(\frac{e^{i\|\underline{p}\|(x^0-y^0)}}{e^{\beta(p_1)\|\underline{p}\|} - 1} - \frac{e^{-i\|\underline{p}\|(x^0-y^0)}}{e^{-\beta(-p_1)\|\underline{p}\|} - 1} \right) d^3\underline{p} \quad (2.8)$$

for $\underline{p} = (p_1, p_2, p_3) \in \mathbb{R}^3$, where

$$\beta(p_1) := \Theta(p_1)\beta_L + \Theta(-p_1)\beta_R \quad (2.9)$$

for the Heaviside function Θ (indicator function of $(0, \infty)$).

As W_N coincides with the β -KMS two-point function W_β (Eq. (2.7)) if $\beta_L = \beta_R =: \beta$, we have to assume that $\beta_L \neq \beta_R$ to obtain a proper NESS. Then there exists a heat (or energy) flow that travels from $x^1 = -\infty$ to $x^1 = +\infty$ for $\beta_L^{-1} > \beta_R^{-1}$ (and reversed for $\beta_L^{-1} < \beta_R^{-1}$), represented by the non-vanishing (01) component of the expected stress-energy tensor [DLSB15] (see Lemma D.2). As noted in [HV18], the NESS agrees with the one constructed in [DLSB15], where the authors assumed the initial heat baths to be in sharp contact at $x^1 = 0$. The smooth transition region in the initial configuration of the system described above guarantees an initial state that satisfies the Hadamard condition everywhere, which enables the construction of NESS in interacting Klein-Gordon models [HV18]. The resulting NESS does not depend on β' (and its chemical potential) as long as the conditions laid out in [HV18, Sec. 3.1] are fulfilled (see [HV18, Thm. 3.2 (1)]). The NESS ω_N is a Hadamard state, i.e. $\widetilde{W}_N := W_N - W_{\text{vac}}$ is a smooth function on $\mathbb{M} \times \mathbb{M}$, given by (using Eqs. (2.5) & (2.8))

$$\widetilde{W}_N(x, y) = \frac{1}{(2\pi)^3} \int_{\mathbb{R}^3} \frac{1}{2\|\underline{p}\|} e^{i\underline{p} \cdot (\underline{x} - \underline{y})} \left(\frac{e^{i\|\underline{p}\|(x^0 - y^0)}}{e^{\beta(p_1)\|\underline{p}\|} - 1} + \frac{e^{-i\|\underline{p}\|(x^0 - y^0)}}{e^{\beta(-p_1)\|\underline{p}\|} - 1} \right) d^3\underline{p}. \quad (2.10)$$

3. Transition rates in (non-)equilibrium states

We fix an inertial reference frame I (the laboratory frame) corresponding to coordinates (x^0, x^1, x^2, x^3) on $\mathbb{M} \cong \mathbb{R}^4$. The inertial time evolution in this frame is implemented on the observable algebra of the scalar field by the *-automorphism group α defined in Eq. (2.1). Let I_v be the inertial reference frame that moves relative to $I \equiv I_0$ with constant velocity $\mathbf{v} \in (-1, 1)$ along the x^1 -axis (which is the longitudinal axis of the NESS specified in Section 2.3). In proper time $\tau \in \mathbb{R}$ the worldline of the detector at rest in I_v (passing through the origin at $\tau = 0$) is, expressed in I ,

$$\tau \mapsto \mathbf{x}_v(\tau) = \gamma(\tau, \mathbf{v}\tau, 0, 0), \quad \gamma := \frac{1}{\sqrt{1 - \mathbf{v}^2}}. \quad (3.1)$$

For later reference we also define the quantities

$$\mathbf{d}_\pm := \gamma(1 \pm \mathbf{v}) = \sqrt{\frac{1 \pm \mathbf{v}}{1 \mp \mathbf{v}}}, \quad (3.2)$$

which represent the Doppler factors for blueshift (+) and redshift (-).

We consider the following two classes of scenarios for the detector-field system.

(KMS- \mathbf{v}) The detector is stationary in $I_{\mathbf{v}}$ and is coupled to a thermal equilibrium state relative to I (the quasi-free KMS state ω_{β} with respect to α at inverse temperature $\beta > 0$, with two-point function given by Eq. (2.7)).

(NESS- \mathbf{v}) The detector is stationary in $I_{\mathbf{v}}$ and is coupled to a NESS in I (the quasi-free Hadamard NESS ω_N with respect to α , with initial semi-infinite heat baths at inverse temperatures $\beta_L, \beta_R > 0$, $\beta_L \neq \beta_R$, and two-point function given by Eq. (2.8)).

As announced in Section 3 we will calculate the transition rates by splitting off the vacuum contribution. The Minkowski vacuum state is a ground state relative to every inertial frame, and the vacuum two-point function W_{vac} is Lorentz-invariant and thus (cf. Eq. (2.6))

$$W_{\text{vac}}(\mathbf{x}_{\mathbf{v}}(s), 0) = W_{\text{vac}}(\mathbf{x}_0(s), 0) = -\frac{1}{4\pi^2} \lim_{\epsilon \rightarrow 0^+} \frac{1}{(s - i\epsilon)^2}$$

for every velocity \mathbf{v} . The vacuum transition rate \mathcal{R}_{vac} is shown to be

$$\mathcal{R}_{\text{vac}}(E) := \int_{\mathbb{R}} e^{-iEs} W_{\text{vac}}(\mathbf{x}_{\mathbf{v}}(s), 0) ds = -\frac{E}{2\pi} \Theta(-E) \quad (3.3)$$

for $E \in \mathbb{R} \setminus \{0\}$ by contour integration (see, e.g., [Sch04], and also [BPPL24]). As expected, the transition rate vanishes for $E > 0$, i.e. there is no detector excitation in the vacuum.

3.1. Detector moving inertially through a heat bath

Let us first consider the scenario (KMS- \mathbf{v}). If the field is prepared in the β -KMS state ω_{β} and the detector moves along the inertial worldline $\mathbf{x}_{\mathbf{v}}$ with constant non-zero velocity \mathbf{v} , the transition rate is [CM95a, CM95b]

$$\mathcal{R}_{\mathbf{v}}^{(\beta)}(E) = \frac{1}{4\pi\beta\gamma_{\mathbf{v}}} \ln \left(\frac{1 - e^{-\beta\mathbf{a}_+ E}}{1 - e^{-\beta\mathbf{a}_- E}} \right) \quad (3.4)$$

for $E \in \mathbb{R} \setminus \{0\}$, where we write $\mathcal{R}_{\mathbf{v}}^{(\beta)} := \mathcal{R}_{\omega_{\beta}}$ for the transition rate (defined in Eq. (2.4)) to highlight the dependence on \mathbf{v} . The expression reveals the relativistic Doppler shift [Rin77] of the radiation perceived by the detector. We provide a derivation of Eq. (3.4) in Appendix A. For small energy gaps,

$$\mathcal{R}_{\mathbf{v}}^{(\beta)}(E) = \frac{\sqrt{1 - \mathbf{v}^2}}{4\pi\beta\mathbf{v}} \ln \left(\frac{1 + \mathbf{v}}{1 - \mathbf{v}} \right) - \frac{E}{4\pi} + \mathcal{O}(E^2). \quad (3.5)$$

Some properties of the transition rate for $E > 0$ can be extracted from Figure 1. In particular, as the velocity increases, the Doppler shift eventually prevents the response of the detector, so that $\mathcal{R}_{\mathbf{v}}^{(\beta)}$ vanishes pointwise as $|\mathbf{v}| \rightarrow 1$ [CM95b]. In the context of an experimental verification of the Unruh effect [Unr76, CHM08] this contributes to the conclusion that for a

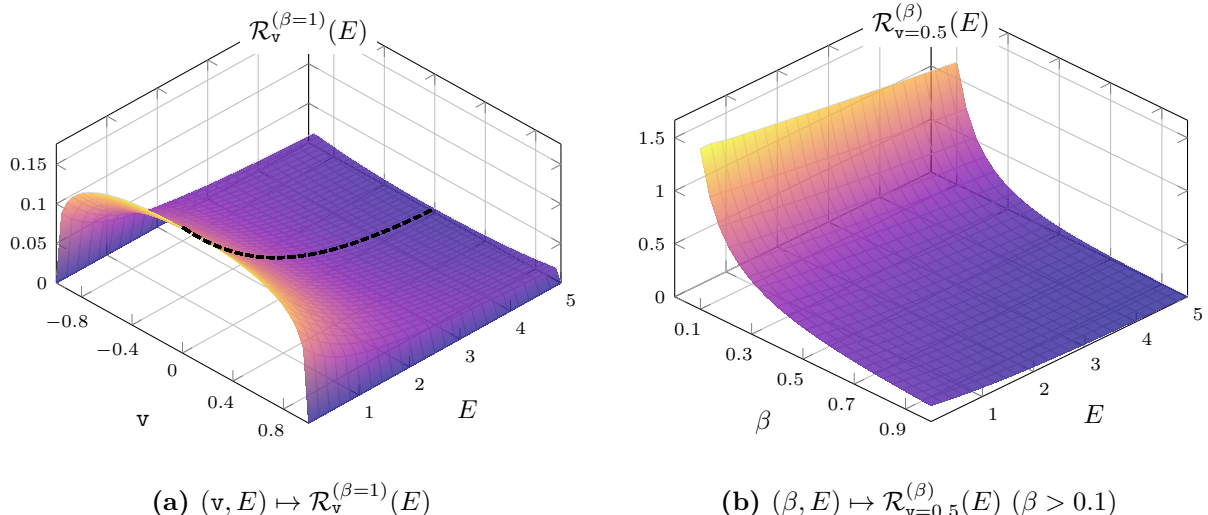


Figure 1: (a) Surface plot of $(v, E) \mapsto \mathcal{R}_v^{(\beta)}(E)$ for fixed $\beta = 1$ and $v \in (-1, 1)$, $E > 0$. The transition rate $\mathcal{R}_v^{(\beta)}(E)$ is given by Eq. (3.4) and is even in v , i.e. $\mathcal{R}_{-v}^{(\beta)} = \mathcal{R}_v^{(\beta)}$. For non-negative v the plot reproduces Fig. 1 in [CM95b]. The maximum of $v \mapsto \mathcal{R}_v^{(\beta)}(E)$ shifts from $v = 0$ for $E \ll \beta^{-1} = 1$ to non-zero $|v| > 0$ for $E \gg \beta^{-1} = 1$; see [CM95b] for a discussion (and also the dashed lines in Figure 4b, where this can be seen more clearly). The dashed surface curve at $v = 0$ represents the transition rate of a stationary detector and is given by the Planckian $\mathcal{R}_0^{(\beta=1)}$ (Eq. (3.6)). (b) Surface plot of $(\beta, E) \mapsto \mathcal{R}_{v=0.5}^{(\beta)}(E)$ for fixed $v = 0.5$ and $\beta > 0.1$, $E > 0$.

uniformly accelerating detector in a background thermal bath the influence of the latter is suppressed for sufficiently high accelerations [CM95a]. The non-Planckian form of $\mathcal{R}_v^{(\beta)}$ has been argued to prove the lack of a continuous Lorentz transformation law for temperature [LM96, LM04] (which found a model-independent corroboration at the level of KMS states in [Sew08, Sew09]; see also [PV25] for related remarks).

In the limit $v \rightarrow 0$, approaching the case (KMS-0) of a detector at rest relative to the reference frame of the thermal equilibrium state, one obtains the well-known transition rate

$$\mathcal{R}_0^{(\beta)}(E) = \lim_{v \rightarrow 0} \mathcal{R}_v^{(\beta)}(E) = \frac{1}{2\pi} \frac{|E|}{e^{\beta|E|} - 1} - \frac{E}{2\pi} \Theta(-E) \equiv \frac{1}{2\pi} \frac{E}{e^{\beta E} - 1} \quad (3.6)$$

corresponding to a Planck (black body) spectrum at the temperature β^{-1} [CM95a, CM95b, Cos04]. Notice that in the zero temperature limit $\beta \rightarrow \infty$ the vacuum transition rate (Eq. (3.3)) is recovered.

3.2. Stationary detector coupled to a NESS

We now turn to the scenario (NESS- v). From Eq. (2.8) we notice that $W_N(\mathbf{x}_v(\tau), \mathbf{x}_v(\tau')) = W_N(\mathbf{x}_v(\tau - \tau'), 0)$ for all $\tau, \tau' \in \mathbb{R}$ (so Eq. (2.4) for the transition rate applies). Define

$$w_{N,v}(s) := W_N(\mathbf{x}_v(s), 0), \quad \tilde{w}_{N,v}(s) := \widetilde{W}_N(\mathbf{x}_v(s), 0) \equiv (W_N - W_{\text{vac}})(\mathbf{x}_v(s), 0).$$

Let us first consider (NESS-0), i.e. the detector is at rest relative to the frame I of the NESS ω_N to which it is coupled. We have the transition rate (Eq. (2.4))

$$\mathcal{R}_{N,0}^{(\beta_L, \beta_R)}(E) := \int_{\mathbb{R}} e^{-iEs} w_{N,0}(s) ds = \int_{\mathbb{R}} e^{-iEs} \tilde{w}_{N,0}(s) ds - \frac{E}{2\pi} \Theta(-E) \quad (3.7)$$

by Eq. (3.3). From Eq. (2.10) we get

$$\tilde{w}_{N,0}(s) = \frac{1}{(2\pi)^3} \int_{\mathbb{R}^3} \frac{1}{2\|\underline{p}\|} \left(\frac{e^{i\|\underline{p}\|s}}{e^{\beta(p_1)\|\underline{p}\|} - 1} + \frac{e^{-i\|\underline{p}\|s}}{e^{\beta(-p_1)\|\underline{p}\|} - 1} \right) d^3\underline{p}$$

for $s \in \mathbb{R}$. Going to spherical coordinates this can be written as the sum of two integrals of the form $\int_0^\infty e^{irs} \frac{r}{e^{\beta r} - 1} dr$, which converges for any $\beta > 0$ and $s \in \mathbb{R}$ (see [EMOT54, Sec. 1.4, (8)] and [Obe90, Sec. 2.3, 3.13] for the Fourier cosine and sine part, respectively). Substituting $p_1 \mapsto -p_1$ in the second term and using the definition of $\beta(p_1)$ (Eq. (2.9)),

$$\begin{aligned} \tilde{w}_{N,0}(s) &= \frac{1}{(2\pi)^3} \int_{\mathbb{R}^3} \frac{1}{\|\underline{p}\|} \frac{\cos(\|\underline{p}\|s)}{e^{\beta(p_1)\|\underline{p}\|} - 1} d^3\underline{p} = \\ &= \frac{1}{(2\pi)^3} \int_{\{p_1 > 0\} \times \mathbb{R}^2} \frac{1}{\|\underline{p}\|} \frac{\cos(\|\underline{p}\|s)}{e^{\beta_L \|\underline{p}\|} - 1} d^3\underline{p} + \frac{1}{(2\pi)^3} \int_{\{p_1 < 0\} \times \mathbb{R}^2} \frac{1}{\|\underline{p}\|} \frac{\cos(\|\underline{p}\|s)}{e^{\beta_R \|\underline{p}\|} - 1} d^3\underline{p} = \\ &= \frac{1}{4\pi^2} (C_{\beta_L}(s) + C_{\beta_R}(s)), \end{aligned} \quad (3.8)$$

where

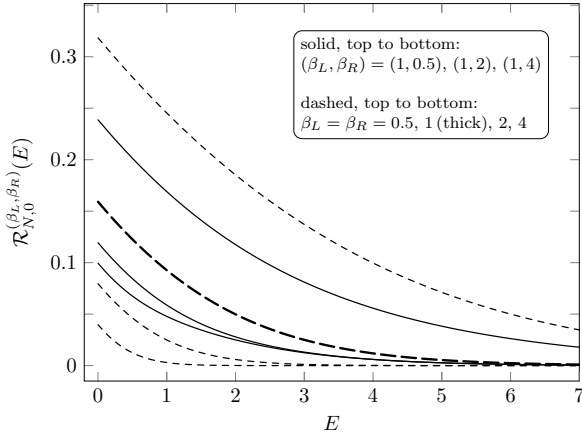
$$C_\beta(s) := \int_0^\infty \frac{r \cos(rs)}{e^{\beta r} - 1} dr = \frac{1}{2s^2} - \frac{\pi^2}{2\beta^2} \frac{1}{\sinh^2\left(\frac{\pi s}{\beta}\right)}, \quad \beta > 0, s \in \mathbb{R},$$

and spherical coordinates on the half-spaces are used, with the integrals over the angular coordinates each giving a factor of 2π . The final expression for C_β is obtained from [EMOT54, Sec. 1.4, (8)] and is to be understood as its smooth continuation to all of \mathbb{R} with $\lim_{s \rightarrow 0} C_\beta(s) = \frac{\pi^2}{6\beta^2} = C_\beta(0)$ (see [EMOT54, Sec. 6.3, (7)]).

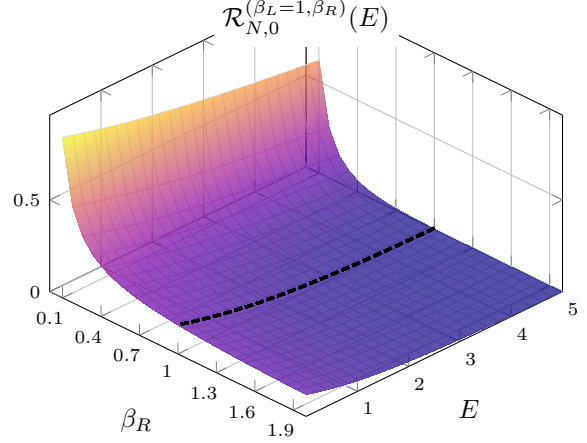
Since $C_\beta \in L^1(\mathbb{R})$ the Fourier cosine transform that defines C_β can be inverted, giving $\int_0^\infty \cos(qs) C_\beta(s) ds = \frac{\pi}{2} q (e^{\beta q} - 1)^{-1}$ for $\beta, q > 0$. The function $\tilde{w}_{N,0}$ is even, so the exponential in the Fourier transform in Eq. (3.7) can be replaced by $\cos(Es) = \cos(|E|s)$. It follows that

$$\begin{aligned} \mathcal{R}_{N,0}^{(\beta_L, \beta_R)}(E) &= 2 \int_0^\infty \cos(|E|s) \tilde{w}_{N,0}(s) ds - \frac{E}{2\pi} \Theta(-E) = \\ &= \frac{1}{4\pi} \left(\frac{|E|}{e^{\beta_L |E|} - 1} + \frac{|E|}{e^{\beta_R |E|} - 1} \right) - \frac{E}{2\pi} \Theta(-E) = \frac{1}{2} \left(\mathcal{R}_0^{(\beta_L)}(E) + \mathcal{R}_0^{(\beta_R)}(E) \right), \end{aligned} \quad (3.9)$$

which is the arithmetic mean of the transition rates for the two initial semi-infinite heat baths



(a) $\mathcal{R}_{N,0}^{(\beta_L=1, \beta_R)}$ (solid) and $\mathcal{R}_0^{(\beta)}$ (dashed)



(b) $(\beta_R, E) \mapsto \mathcal{R}_{N,0}^{(\beta_L=1, \beta_R)}(E)$ ($\beta_R > 0.1$)

Figure 2: (a) Plot of the transition rate $\mathcal{R}_{N,0}^{(\beta_L, \beta_R)}$, given by Eq. (3.9), for $E > 0$, fixed $\beta_L = 1$, and different values of β_R (solid), in comparison with the Planckian transition rates $\mathcal{R}_0^{(\beta)}$ (Eq. (3.6)) for β from the same set as β_R (dashed). The rate $\mathcal{R}_0^{(\beta=1)}$, which equals $\mathcal{R}_{N,0}^{(\beta_L=1, \beta_R=1)}$, is highlighted as thick dashed line. (b) Surface plot of $(\beta_R, E) \mapsto \mathcal{R}_{N,0}^{(\beta_L, \beta_R)}(E)$ for fixed $\beta_L = 1$ and $\beta_R > 0.1$. The dashed surface curve at $\beta_R = 1$ represents the Planckian $\mathcal{R}_0^{(\beta=1)}$.

at inverse temperatures β_L, β_R , given by Eq. (3.6).

For $\beta_L = \beta_R =: \beta$ the transition rate $\mathcal{R}_{N,0}^{(\beta_L, \beta_R)}$ equals the Planckian $\mathcal{R}_0^{(\beta)}$, as expected. For a proper NESS with $\beta_L \neq \beta_R$, however, the detector is excited by modes coming from $x^1 = -\infty$ and $x^1 = \infty$ with Planck spectrum of temperature β_L^{-1} and β_R^{-1} , respectively. The detector, which is at rest relative to the two heat baths, effectively reacts to a mixture of the corresponding KMS states. If the transition spectrum is sampled for a sufficiently large set of detector energies E , one will always find a non-thermal detector response (i.e. not corresponding to a Planck spectrum). Figure 2 shows plots of $\mathcal{R}_{N,0}^{(\beta_L, \beta_R)}$ for fixed $\beta_L = 1$ and different values of β_R when $E > 0$. Irrespective of β_L, β_R , the transition rate vanishes as $E \rightarrow \infty$ and is asymptotic to the function $E \mapsto -\frac{E}{2\pi}$ as $E \rightarrow -\infty$, i.e. $\lim_{E \rightarrow -\infty} (\mathcal{R}_{N,0}^{(\beta_L, \beta_R)}(E) + \frac{E}{2\pi}) = 0$.

3.3. Detector moving inertially through a NESS

Consider the case (NESS- \mathbf{v}) for $\mathbf{v} \in (-1, 1) \setminus \{0\}$, that is, the detector couples to ω_N and travels along the inertial worldline $\mathbf{x}_{\mathbf{v}}$ (Eq. (3.1)) with constant non-zero velocity \mathbf{v} . As $\underline{p} \cdot \underline{x}_{\mathbf{v}}(s) = p_1 \gamma \mathbf{v} s$, Eq. (2.10) implies

$$\tilde{w}_{N, \mathbf{v}}(s) := \tilde{W}_N(\mathbf{x}_{\mathbf{v}}(s), 0) = \frac{1}{(2\pi)^3} \int_{\mathbb{R}^3} \frac{1}{2\|\underline{p}\|} \left(\frac{e^{ip_1 \gamma \mathbf{v} s} e^{i\|\underline{p}\| \gamma s}}{e^{\beta(p_1) \|\underline{p}\|} - 1} + \frac{e^{ip_1 \gamma \mathbf{v} s} e^{-i\|\underline{p}\| \gamma s}}{e^{\beta(-p_1) \|\underline{p}\|} - 1} \right) d^3 \underline{p}, \quad (3.10)$$

and substituting $p_1 \mapsto -p_1$ in the second term yields

$$\tilde{w}_{N,\mathbf{v}}(s) = \frac{1}{(2\pi)^3} \int_{\mathbb{R}^3} \frac{1}{\|\underline{p}\|} \frac{\cos(p_1 \gamma \mathbf{v} s + \|\underline{p}\| \gamma s)}{e^{\beta(p_1) \|\underline{p}\|} - 1} d^3 \underline{p}. \quad (3.11)$$

This integral is split into a sum according to the definition of $\beta(p_1)$ (Eq. (2.9)). Choosing spherical coordinates with θ the polar angle from the polar axis placed along the positive x^1 -axis one finds by Eq. (A.4)

$$\begin{aligned} \int_{\{p_1 > 0\} \times \mathbb{R}^2} \frac{1}{\|\underline{p}\|} \frac{\cos(p_1 \gamma \mathbf{v} s + \|\underline{p}\| \gamma s)}{e^{\beta(p_1) \|\underline{p}\|} - 1} d^3 \underline{p} &= \\ &= 2\pi \int_0^\infty \int_0^{\pi/2} \frac{r \cos(\gamma \mathbf{v} s r \cos(\theta) + \gamma s r)}{e^{\beta_L r} - 1} \sin(\theta) d\theta dr = \\ &= \frac{2\pi}{\gamma \mathbf{v} s} \int_0^\infty \frac{\sin(\gamma(1+\mathbf{v})sr) - \sin(\gamma sr)}{e^{\beta_L r} - 1} dr = \\ &= \frac{2\pi}{\gamma \mathbf{v} s} \left[-\frac{\mathbf{d}_-}{2s} + \frac{\pi}{2\beta_L} \coth\left(\frac{\pi s}{\beta_L \mathbf{d}_-}\right) + \frac{1}{2\gamma s} - \frac{\pi}{2\beta_L} \coth\left(\frac{\pi \gamma s}{\beta_L}\right) \right] \end{aligned} \quad (3.12)$$

for the Doppler factors \mathbf{d}_\pm (Eq. (3.2)). Similarly,

$$\begin{aligned} \int_{\{p_1 < 0\} \times \mathbb{R}^2} \frac{1}{\|\underline{p}\|} \frac{\cos(p_1 \gamma \mathbf{v} s + \|\underline{p}\| \gamma s)}{e^{\beta(p_1) \|\underline{p}\|} - 1} d^3 \underline{p} &= \\ &= 2\pi \int_0^\infty \int_{\pi/2}^\pi \frac{r \cos(\gamma \mathbf{v} s r \cos(\theta) + \gamma s r)}{e^{\beta_R r} - 1} \sin(\theta) d\theta dr = \\ &= -\frac{2\pi}{\gamma \mathbf{v} s} \left[-\frac{\mathbf{d}_+}{2s} + \frac{\pi}{2\beta_R} \coth\left(\frac{\pi s}{\beta_R \mathbf{d}_+}\right) + \frac{1}{2\gamma s} - \frac{\pi}{2\beta_R} \coth\left(\frac{\pi \gamma s}{\beta_R}\right) \right]. \end{aligned} \quad (3.13)$$

Taking the sum of (3.12) and (3.13) and using $\mathbf{d}_+ - \mathbf{d}_- = 2\gamma \mathbf{v}$, Eq. (3.11) becomes

$$\begin{aligned} \tilde{w}_{N,\mathbf{v}}(s) &= \frac{1}{4\pi^2 s^2} + \\ &+ \frac{1}{8\pi \gamma \mathbf{v} \beta_L s} \left[\coth\left(\frac{\pi s}{\beta_L \mathbf{d}_-}\right) - \coth\left(\frac{\pi \gamma s}{\beta_L}\right) \right] - \frac{1}{8\pi \gamma \mathbf{v} \beta_R s} \left[\coth\left(\frac{\pi s}{\beta_R \mathbf{d}_+}\right) - \coth\left(\frac{\pi \gamma s}{\beta_R}\right) \right] \\ &= \frac{1}{4\pi \gamma \mathbf{v}} \left[\frac{1}{\beta_L} (f_{\beta_L/\gamma}(s) - f_{\beta_L \mathbf{d}_-}(s)) - \frac{1}{\beta_R} (f_{\beta_R/\gamma}(s) - f_{\beta_R \mathbf{d}_+}(s)) \right] \end{aligned} \quad (3.14)$$

for the smooth function f_c ($c > 0$) defined in Eq. (A.8). An alternative derivation is presented in Appendix B. For $\beta_L = \beta_R =: \beta > 0$, Eq. (3.14) reduces to Eq. (A.7) (case (KMS-v)). Furthermore, for any $\beta_L, \beta_R > 0$, one regains Eq. (3.8) in the limit $\mathbf{v} \rightarrow 0$ (case (NESS-0)).

Eqs. (3.3), (3.14) & (A.9) imply that the transition rate for (NESS-v) is given by

$$\mathcal{R}_{N,\mathbf{v}}^{(\beta_L, \beta_R)}(E) := \int_{\mathbb{R}} e^{-iEs} w_{N,\mathbf{v}}(s) ds = \int_{\mathbb{R}} e^{-iEs} \tilde{w}_{N,\mathbf{v}}(s) ds - \frac{E}{2\pi} \Theta(-E) =$$

$$\begin{aligned}
&= \frac{1}{4\pi\gamma\mathbf{v}} \left[\frac{1}{\beta_L} \ln \left(\frac{1 - e^{-\beta_L|E|/\gamma}}{1 - e^{-\beta_L\mathbf{d}_-|E|}} \right) - \frac{1}{\beta_R} \ln \left(\frac{1 - e^{-\beta_R|E|/\gamma}}{1 - e^{-\beta_R\mathbf{d}_+|E|}} \right) \right] - \frac{E}{2\pi} \Theta(-E) = \\
&= \frac{1}{4\pi\gamma\mathbf{v}} \left[\frac{1}{\beta_L} \ln \left(\frac{1 - e^{-\beta_L E/\gamma}}{1 - e^{-\beta_L\mathbf{d}_- E}} \right) - \frac{1}{\beta_R} \ln \left(\frac{1 - e^{-\beta_R E/\gamma}}{1 - e^{-\beta_R\mathbf{d}_+ E}} \right) \right] \\
&= R(\beta_L, \mathbf{v}, E) + R(\beta_R, -\mathbf{v}, E),
\end{aligned} \tag{3.15}$$

where the Heaviside function term is absorbed by some rearrangements (similar to Eq. (A.10)), and we defined

$$R(\beta, \mathbf{v}, E) := \frac{\sqrt{1 - \mathbf{v}^2}}{4\pi\mathbf{v}\beta} \ln \left(\frac{1 - e^{-\beta\sqrt{1 - \mathbf{v}^2}E}}{1 - e^{-\beta\sqrt{\frac{1 - \mathbf{v}}{1 + \mathbf{v}}}}E}} \right) \tag{3.16}$$

for $\beta > 0$, $\mathbf{v} \in (-1, 1) \setminus \{0\}$, $E \in \mathbb{R} \setminus \{0\}$. A Taylor expansion in E yields

$$\mathcal{R}_{N,\mathbf{v}}^{(\beta_L, \beta_R)}(E) = \frac{\sqrt{1 - \mathbf{v}^2}}{4\pi\mathbf{v}} \left(\frac{1}{\beta_L} \ln(1 + \mathbf{v}) - \frac{1}{\beta_R} \ln(1 - \mathbf{v}) \right) - \frac{E}{4\pi} + \mathcal{O}(E^2). \tag{3.17}$$

The motion of the detector along the x^1 -axis with velocity $\mathbf{v} \neq 0$ relative to the two semi-infinite heat baths results in a transition rate $\mathcal{R}_{N,\mathbf{v}}^{(\beta_L, \beta_R)}$ that deviates from the mean transition rate $\mathcal{R}_{N,0}^{(\beta_L, \beta_R)} = \lim_{\mathbf{v} \rightarrow 0} \mathcal{R}_{N,\mathbf{v}}^{(\beta_L, \beta_R)}$ corresponding to the individual β_L - and β_R -KMS states (Eq. (3.9)). One can interpret this behavior to be similar to the case (KMS- \mathbf{v}) of a detector moving with constant velocity relative to an inertial KMS state (Section 3.1). In contrast to $\mathcal{R}_{\mathbf{v}}^{(\beta)}$ (Eq. (3.4)), however, the transition rate $\mathcal{R}_{N,\mathbf{v}}^{(\beta_L, \beta_R)}$ is not an even function of \mathbf{v} unless $\beta_L = \beta_R =: \beta$, in which case the detector interacts with a global β -KMS state and the transition rate reduces to $\mathcal{R}_{N,\mathbf{v}}^{(\beta, \beta)} = \mathcal{R}_{\mathbf{v}}^{(\beta)}$. Moreover, $\mathcal{R}_{N,\mathbf{v}}^{(\beta_L, \beta_R)}$ is not invariant under the exchange of β_L and β_R for non-zero detector velocity and $\beta_L \neq \beta_R$. Hence we find that a relation analogous to Eq. (3.9) does not hold, to wit,

$$\mathcal{R}_{N,\mathbf{v}}^{(\beta_L, \beta_R)} \neq \frac{1}{2} (\mathcal{R}_{\mathbf{v}}^{(\beta_L)} + \mathcal{R}_{\mathbf{v}}^{(\beta_R)}) , \quad \mathbf{v} \in (-1, 1) \setminus \{0\}, \quad \beta_L \neq \beta_R$$

for $\mathcal{R}_{\mathbf{v}}^{(\beta)}$ given by Eq. (3.4). However, the transition rate $\mathcal{R}_{N,\mathbf{v}}^{(\beta_L, \beta_R)}$ is invariant under simultaneously exchanging the β_L - and β_R -KMS heat baths as well as reversing the direction of motion along the x^1 -axis, i.e. $\mathbf{v} \mapsto -\mathbf{v}$. This behavior is to be expected, because the detector's motion relative to the semi-infinite heat baths distinguishes a direction (determined by the sign of \mathbf{v}) in relation to the thermal gradient of the NESS (determined by the sign of $\beta_R - \beta_L$), manifesting in a Doppler shift as signified by the Doppler factors appearing in Eq. (3.15). No such direction is distinguished in the stationary case (NESS-0); the transition rate incorporates quanta incoming from all spatial directions, making $\mathcal{R}_{N,0}^{(\beta_L, \beta_R)}$ symmetric in β_L, β_R despite the existence of a heat flow.

For the rest of this section we restrict our attention to positive energy gaps $E > 0$. Figure 3 shows the transition rate $\mathcal{R}_{N,\mathbf{v}}^{(\beta_L, \beta_R)}$ as a function of \mathbf{v} for arbitrarily chosen values $\beta_L = 1$,

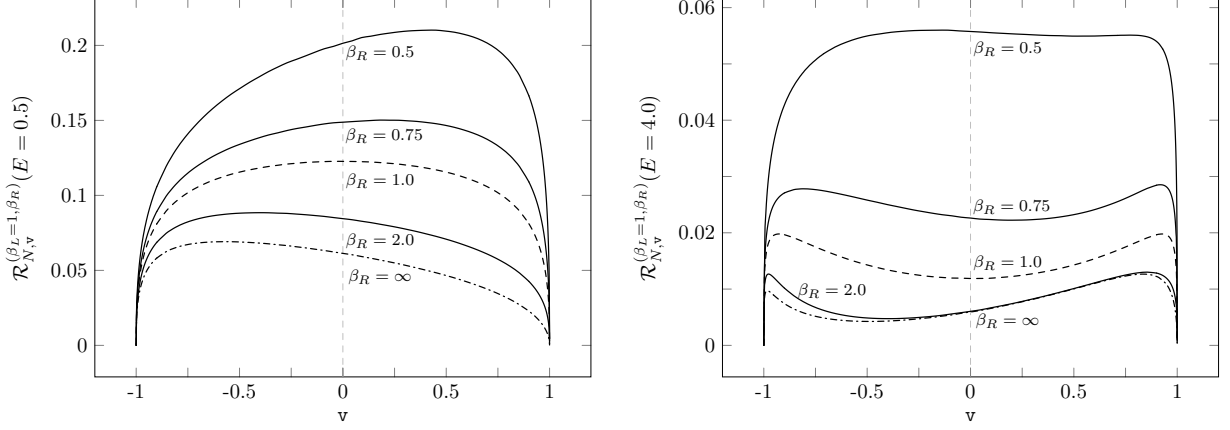


Figure 3: Plot of $\mathcal{R}_{N,v}^{(\beta_L, \beta_R)}(E)$ as a function of v for $\beta_L = 1$, $E = 0.5$ (left) and $E = 4.0$ (right), and different values of β_R . In both plots the dashed line represents $\beta_L = 1 = \beta_R$ and thus the transition rate $\mathcal{R}_v^{(\beta=1)}$ of a KMS heat bath (Eq. (3.4)), and the case $\beta_R = \infty$ is shown by a dash-dotted line.

$\beta_R \in \{0.5, 0.75, 1, 2, \infty\}$, $E \in \{0.5, 4\}$. First of all, we see that $\mathcal{R}_{N,v}^{(\beta_L, \beta_R)}$ vanishes pointwise for $|v| \rightarrow 1$. Following the explanation given in [CM95a, CM95b] for a detector moving in a heat bath, we can interpret this in terms of the Doppler effect gradually shifting the quanta of the surrounding NESS outside the detectable range as $|v|$ approaches the speed of light, thereby impeding the excitation of the detector. The plots also reveal the asymmetry in v for $\beta_L \neq \beta_R$ and fixed E , which reflects the asymmetry under the exchange of the heat baths as noted above. At certain velocities the Doppler shift facilitates the excitation of the detector: For $E = 0.5$ the maximal transition rate is attained for some $v > 0$ when $\beta_R < \beta_L$, and for some $v < 0$ when $\beta_R > \beta_L$. For larger energy gaps, exemplified by the value $E = 4.0$ in Figure 3, the transition rate admits two maxima located towards large $|v|$.

On physical grounds we would expect a combination of Doppler shifts taking effect in the rest frame of the detector, one caused by the detector's motion relative to the laboratory frame, and another caused by the heat flow of the NESS. For $E = 0.5$ we see that $\mathcal{R}_{N,v}^{(\beta_L, \beta_R)}(E)$ peaks when the detector moves against the direction of the heat flow. Considering the isotropic response in the stationary case (NESS-0), we can take the behavior of $\mathcal{R}_{N,v}^{(\beta_L, \beta_R)}$ as an indicator of purely kinematical effects from the presence of the two heat baths. Notice that the asymmetry in v subsides when both semi-infinite heat baths have the same temperature, i.e. when the field is in an inertial KMS state, for which the transition rate takes its maximum at $v = 0$ for sufficiently small $E > 0$ (see the discussion in [CM95a, CM95b]).

Let us now consider the limit case $\beta_R \rightarrow \infty$ for which the right reservoir approaches the ground state (acting as a perfect “heat sink”). (The situation with $\beta_L \rightarrow \infty$ and finite β_R is effectively obtained from this by inverting the direction of motion, $v \mapsto -v$.) Since $\lim_{\beta \rightarrow \infty} R(\beta, v, E) = 0$ for $E > 0$ and $v \in (-1, 1) \setminus \{0\}$ (see Eq. (3.16)), the transition rate in

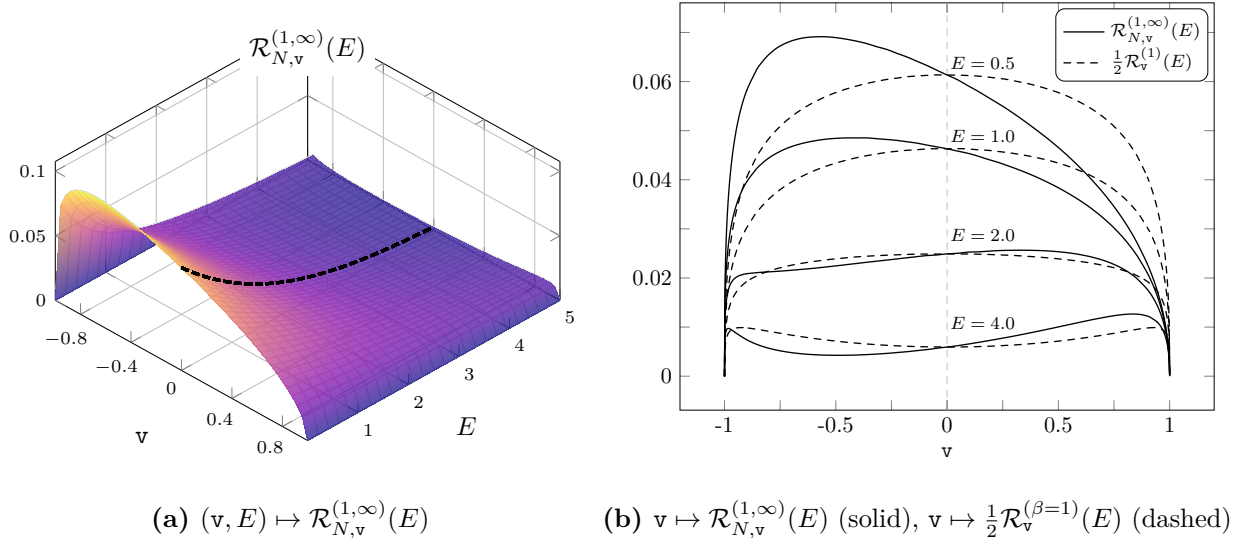


Figure 4: (a) Surface plot of $(v, E) \mapsto \mathcal{R}_{N,v}^{(\beta_L, \infty)}(E)$ for $\beta_L = 1$ and $v \in (-1, 1)$, $E > 0$. The dashed surface curve at $v = 0$ represents the transition rate of a stationary detector and is given by $\frac{1}{2}\mathcal{R}_0^{(1)}$. (b) Plot of the same transition rate as a function of v for different values of $E > 0$ (solid lines). The corresponding rescaled transition rates $\frac{1}{2}\mathcal{R}_v^{(1)}$ for the single 1-KMS heat bath (Eq. (3.4)) are shown as dashed lines.

this limit is given by $R(\beta_L, v, E)$, i.e.

$$\mathcal{R}_{N,v}^{(\beta_L, \infty)}(E) := \lim_{\beta_R \rightarrow \infty} \mathcal{R}_{N,v}^{(\beta_L, \beta_R)}(E) = \frac{\sqrt{1-v^2}}{4\pi v \beta_L} \ln \left(\frac{1 - e^{-\beta_L E \sqrt{1-v^2}}}{1 - e^{-\beta_L E \sqrt{\frac{1-v}{1+v}}}} \right), \quad \beta_L, E > 0.$$

The plots in Figure 4 visualize this transition rate (for $\beta_L = 1$). For every fixed v and β_L , the function $\mathcal{R}_{N,v}^{(\beta_L, \infty)}$ is given by $\sqrt{1-v^2}(4\pi v \beta_L)^{-1} \ln(1+v)$ in the limit $E \rightarrow 0$ (see Eq. (3.17)), and is decreasing in $E > 0$.

We can compare the transition rate with the scenario (KMS- v) in which the Minkowski vacuum state (and thus the heat flow to $x^1 = \infty$) is absent and the detector only interacts with a global β_L -KMS heat bath. To this end, we consider in Figure 4b the rescaled transition rate $\frac{1}{2}\mathcal{R}_v^{(\beta_L)}$ (Eq. (3.4)), where the factor $\frac{1}{2}$ accommodates for the limit $v \rightarrow 0$ in which $\mathcal{R}_{N,0}^{(\beta_L, \infty)}(E) = \frac{1}{2}\mathcal{R}_0^{(\beta_L)}(E)$ for $E > 0$ by Eq. (3.9). The relation between Figure 4 and Figure 1a shows the asymmetry in v discussed above.

For a comparison with the case (NESS-0) we examine the quotient

$$\frac{\mathcal{R}_{N,v}^{(\beta_L, \infty)}(E)}{\mathcal{R}_{N,0}^{(\beta_L, \infty)}(E)} = \frac{\sqrt{1-v^2}(e^{\beta_L E} - 1)}{v \beta_L E} \ln \left(\frac{1 - e^{-\beta_L E \sqrt{1-v^2}}}{1 - e^{-\beta_L E \sqrt{\frac{1-v}{1+v}}}} \right), \quad \beta_L, E > 0$$

as a function of $v \in (-1, 1)$ parametrized by $\beta_L E > 0$. In the limit $\beta_L E \rightarrow 0$ this quotient equals $\sqrt{1-v^2} v^{-1} \ln(1+v)$ for every fixed v (cf. Eq. (3.17)). The plots in Figure 5 again show the dependence on the sign of v , in contrast to the analogous quotient $\mathcal{R}_v^{(\beta)}(E)/\mathcal{R}_0^{(\beta)}(E)$ in the case (KMS- v), which is even in v and has been discussed in [Cos04]. As in [Cos04] we

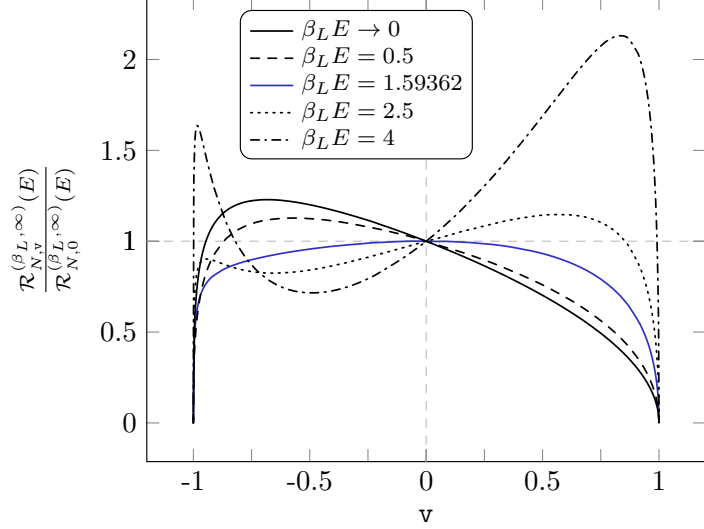


Figure 5: Plots of the quotient of $\mathcal{R}_{N,v}^{(\beta_L, \infty)}(E)$ and $\mathcal{R}_{N,0}^{(\beta_L, \infty)}(E) = \frac{1}{2}\mathcal{R}_0^{(\beta_L)}(E)$ (for $E > 0$) as a function of v in the limit $\beta_L E \rightarrow 0$ (solid) and for $\beta_L E = 0.5$ (dashed), 2.5 (dotted), 4 (dash-dotted), and the critical value $2 + W(-2e^{-2}) \approx 1.59362$ (solid blue).

can find the “critical value” of $\beta_L E > 0$ that determines the change of slope in $v = 0$ that occurs when passing from “smaller” to “larger” values of $\beta_L E$. The first two terms in the Taylor expansion are

$$\frac{\mathcal{R}_{N,v}^{(\beta_L, \infty)}(E)}{\mathcal{R}_{N,0}^{(\beta_L, \infty)}(E)} = 1 + \frac{e^{\beta_L E}(\beta_L E - 2) + 2}{2(e^{\beta_L E} - 1)} v + \mathcal{O}(v^2),$$

so the first derivative of the quotient in $v = 0$ vanishes if $e^{\beta_L E}(\beta_L E - 2) + 2 = 0$. This equation is solved for $\beta_L E = 2 + W(-2e^{-2}) \approx 1.59362$, where W denotes the Lambert W -function [DLMF, 4.13]. At this value of $\beta_L E$ the quotient $\mathcal{R}_{N,v}^{(\beta_L, \infty)}(E)/\mathcal{R}_{N,0}^{(\beta_L, \infty)}(E)$ is smaller than 1 for all $v \in (-1, 1) \setminus \{0\}$ (see Figure 5). In the KMS case the critical value of βE for the corresponding quotient $\mathcal{R}_v^{(\beta)}(E)/\mathcal{R}_0^{(\beta)}(E)$ has been derived in [Cos04]: It is determined by the vanishing second derivative of $\mathcal{R}_v^{(\beta)}(E)/\mathcal{R}_0^{(\beta)}(E)$ in $v = 0$ (note that $\mathcal{R}_v^{(\beta)}$ only depends on even powers of v as a manifestation of symmetry) and is given by the solution to $\beta E \coth(\beta E/2) = 3$, which is approximately 2.57568. Hence the critical value in the NESS case is about 38% less the value in the KMS case.

4. Detailed balance effective temperature

The detailed balance condition [Tak86, FJL16] for the ratio of excitation and de-excitation probabilities of the detector allows to assign an effective temperature [GJMT20, BEG+20,

$$\widehat{T}(E) := \frac{E}{\ln \left(\frac{\mathcal{R}_\omega(-E)}{\mathcal{R}_\omega(E)} \right)},$$

to the response of a detector with energy gap $E \in \mathbb{R} \setminus \{0\}$, i.e. $\widehat{T}(E)$ is the quantity such that $\mathcal{R}_\omega(E) = e^{-E/\widehat{T}(E)} \mathcal{R}_\omega(-E)$ holds for the transition rate \mathcal{R}_ω of the detector coupled to the field state ω (Eq. (2.4)). Notice that $\widehat{T}(-E) = \widehat{T}(E)$ for all $E \in \mathbb{R} \setminus \{0\}$. If ω is a β -KMS state relative to the detector's rest frame (case (KMS-0)) then $\widehat{T}(E)$ is independent of E and coincides with the temperature β^{-1} , as can be seen by inserting $\mathcal{R}_0^{(\beta)}$ from Eq. (3.6). In general, however, the detailed balance effective temperature $\widehat{T}(E)$ will depend on the energy gap of the detector and thus does not represent an equilibrium temperature in the Gibbs sense. While the significance and interpretation of $\widehat{T}(E)$ as a thermodynamic quantity might be up to debate, it nevertheless can serve as a characteristic quantity for the asymptotic readings of the detector for given E under the interaction with the quantum field (see [GJMT20, BEG⁺20, BL23, BPPL24, PL25] for comments and some recent applications, and further references therein). Moreover, in [JM19] it has been shown that the detailed balance effective temperature determines the asymptotic reduced density matrix of the detector under Born-Markov approximation.

Let us denote the effective temperatures for the cases (KMS- \mathbf{v}) and (NESS- \mathbf{v}) by $\widehat{T}_{\mathbf{v}}^{(\beta)}$ and $\widehat{T}_{N,\mathbf{v}}^{(\beta_L,\beta_R)}$ for $\mathbf{v} \in (-1, 1)$, respectively. As noted above, $\widehat{T}_0^{(\beta)} \equiv \beta^{-1}$ for every $\beta > 0$. For $\mathbf{v} \neq 0$, Eqs. (3.4) & (3.5) imply that

$$\widehat{T}_{\mathbf{v}}^{(\beta)}(E) = E \left[\ln \left(\frac{\ln \left(\frac{1 - e^{\beta \mathbf{a}_+ E}}{1 - e^{\beta \mathbf{a}_- E}} \right)}{\ln \left(\frac{1 - e^{-\beta \mathbf{a}_+ E}}{1 - e^{-\beta \mathbf{a}_- E}} \right)} \right) \right]^{-1} = \frac{\sqrt{1 - \mathbf{v}^2}}{2\beta \mathbf{v}} \ln \left(\frac{1 + \mathbf{v}}{1 - \mathbf{v}} \right) + \mathcal{O}(E^2). \quad (4.1)$$

The lowest order of Eq. (4.1) coincides with [LM96, Eq. (8)], the solid angle average of a ‘‘directional temperature’’; see Appendix C for some details. For small $|\mathbf{v}|$ and $|E|$ the detailed balance temperature $\widehat{T}_{\mathbf{v}}^{(\beta)}$ is approximately

$$\widehat{T}_{\mathbf{v}}^{(\beta)}(E) \simeq \beta^{-1} \left(1 - \frac{\mathbf{v}^2}{6} \right), \quad |\mathbf{v}| \ll 1, \quad E \rightarrow 0, \quad (4.2)$$

which is strictly smaller than the rest frame temperature β^{-1} and has been given in [CM95b, Eq. (9)] as the effective temperature defined by a moving observer at small velocities and in the infrared regime of the radiation spectrum. We note that other spectral regimes and velocities relate to differing results, some of which may be higher than the rest frame temperature [CM95b]. This is closely related to the argument in [CM95b, LM96, LM04] against the existence of a relativistic transformation law for temperature (see also [FPM17] and [CJ03, Sec. 7.7] for a review of the various approaches and positions on this matter).

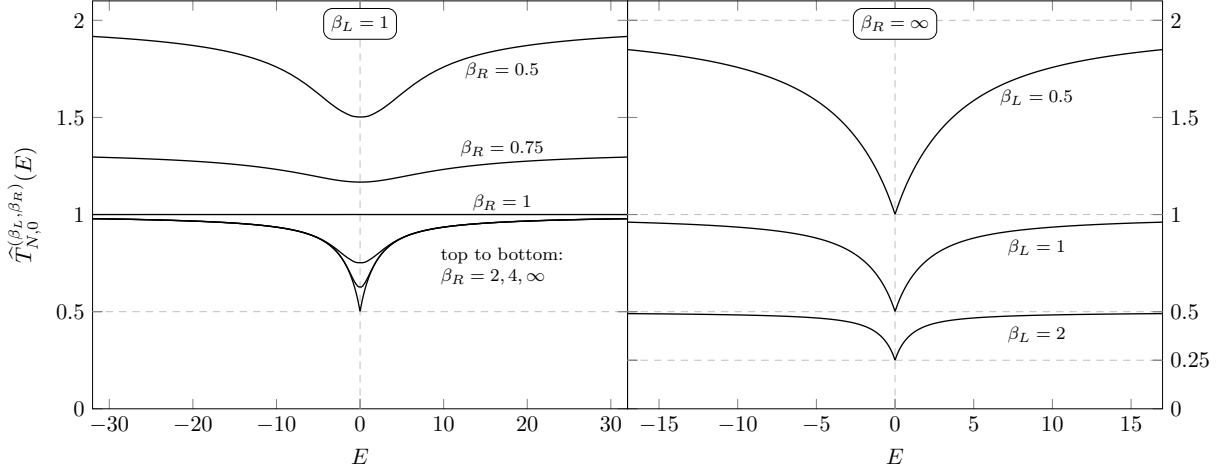


Figure 6: Plot of the effective temperature $\widehat{T}_{N,0}^{(\beta_L, \beta_R)}$, for $\beta_L = 1$ and different values of β_R (left panel), and for $\beta_R = \infty$ and different values of β_L (right panel). This illustrates the limits $\lim_{E \rightarrow 0} \widehat{T}_{N,0}^{(\beta_L, \beta_R)}(E) = (\beta_L^{-1} + \beta_R^{-1})/2$ and $\lim_{|E| \rightarrow \infty} \widehat{T}_{N,0}^{(\beta_L, \beta_R)}(E) = (\min(\beta_L, \beta_R))^{-1}$, with the thermal case $\widehat{T}_{N,0}^{(\beta, \beta)} = \widehat{T}_0^{(\beta)} \equiv \beta^{-1}$ for $\beta > 0$.

We now turn to (NESS-0). Using Eq. (3.9) we find that

$$\widehat{T}_{N,0}^{(\beta_L, \beta_R)}(E) = E \left[\ln \left(\frac{2e^{(\beta_L + \beta_R)E} - e^{\beta_L E} - e^{\beta_R E}}{e^{\beta_L E} + e^{\beta_R E} - 2} \right) \right]^{-1} = \frac{1}{2}(\beta_L^{-1} + \beta_R^{-1}) + \mathcal{O}(E^2), \quad (4.3)$$

with $\widehat{T}_{N,0}^{(\beta, \beta)} = \widehat{T}_0^{(\beta)} \equiv \beta^{-1}$. For $\beta_L > \beta_R$ and $E > 0$,

$$\lim_{E \rightarrow \infty} \frac{1}{E} \ln \left(\frac{2e^{(\beta_L + \beta_R)E} - e^{\beta_L E} - e^{\beta_R E}}{e^{\beta_L E} + e^{\beta_R E} - 2} \right) = \lim_{E \rightarrow \infty} \frac{\ln(2e^{\beta_R E} - 1)}{E} = \beta_R$$

by continuity, so for large $|E|$ the hotter heat bath dominates in the effective temperature:

$$\lim_{|E| \rightarrow \infty} \widehat{T}_{N,0}^{(\beta_L, \beta_R)}(E) = \frac{1}{\min(\beta_L, \beta_R)} \quad (4.4)$$

If one of the heat baths is replaced by the vacuum state, the effective temperature reads

$$\widehat{T}_{N,0}^{(\beta_L, \infty)}(E) := \lim_{\beta_R \rightarrow \infty} \widehat{T}_{N,0}^{(\beta_L, \beta_R)}(E) = \frac{|E|}{\ln(2e^{\beta_L |E|} - 1)} = \frac{1}{2\beta_L} + \frac{|E|}{4} + \mathcal{O}(E^2)$$

for all $\beta_L > 0$ and $E \neq 0$. For $E \rightarrow 0$ the effective temperature $\widehat{T}_{N,0}^{(\beta_L, \infty)}(E)$ approaches $(2\beta_L)^{-1}$, while for $|E| \rightarrow \infty$ it approaches β_L^{-1} (cf. Eq. (4.4)). The functional properties of $\widehat{T}_{N,0}^{(\beta_L, \beta_R)}$ are illustrated in Figures 6 & 7. Once again, we see that the response of a stationary detector in the NESS does not correspond to a thermal equilibrium in the Gibbs sense (cf. the paragraph below Eq. (3.9)).

The detailed balance effective temperature $\widehat{T}_{N,v}^{(\beta_L, \beta_R)}$ for (NESS-v) is obtained from Eq. (3.15).

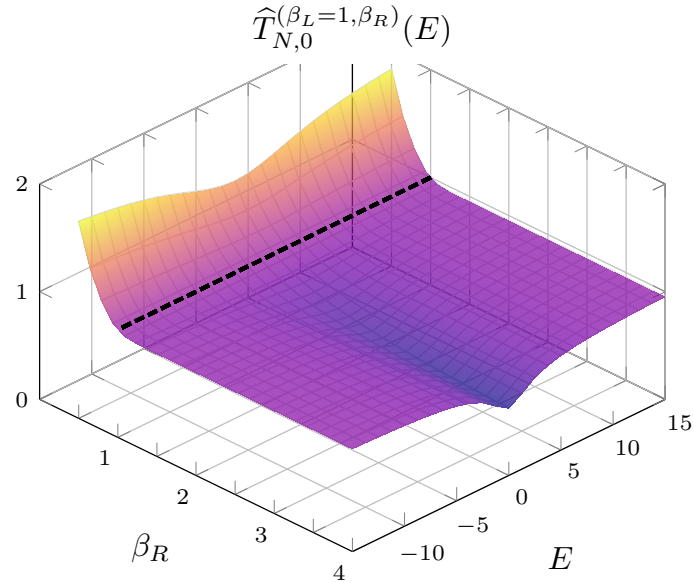


Figure 7: Surface plot of $(\beta_R, E) \mapsto \widehat{T}_{N,0}^{(\beta_L, \beta_R)}(E)$ for $\beta_L = 1$ and $\beta_R > 0.5$, corresponding to the left panel in Figure 6. The dashed surface curve at $\beta_R = \beta_L = 1$ represents the constant KMS heat bath temperature $\widehat{T}_0^{(1)} = 1$ (as a consequence of $\mathcal{R}_{N,0}^{(\beta, \beta)} = \mathcal{R}_0^{(\beta)}$).

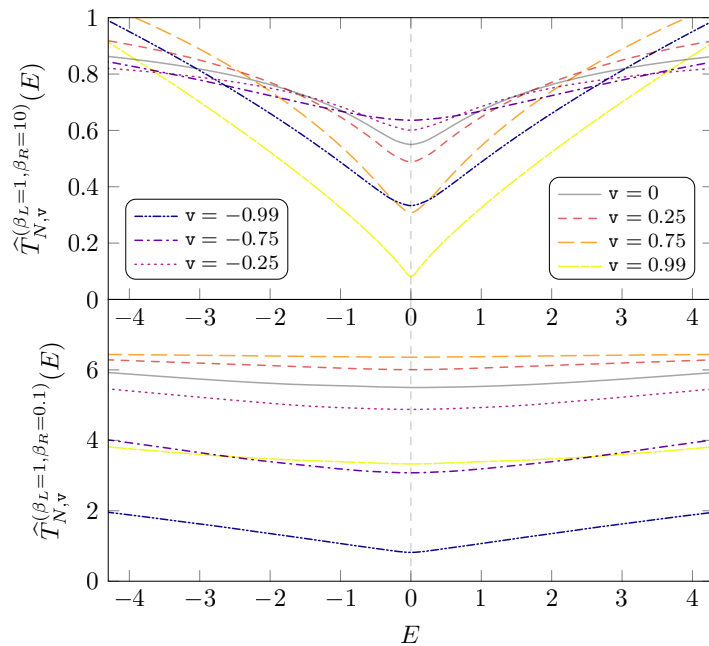
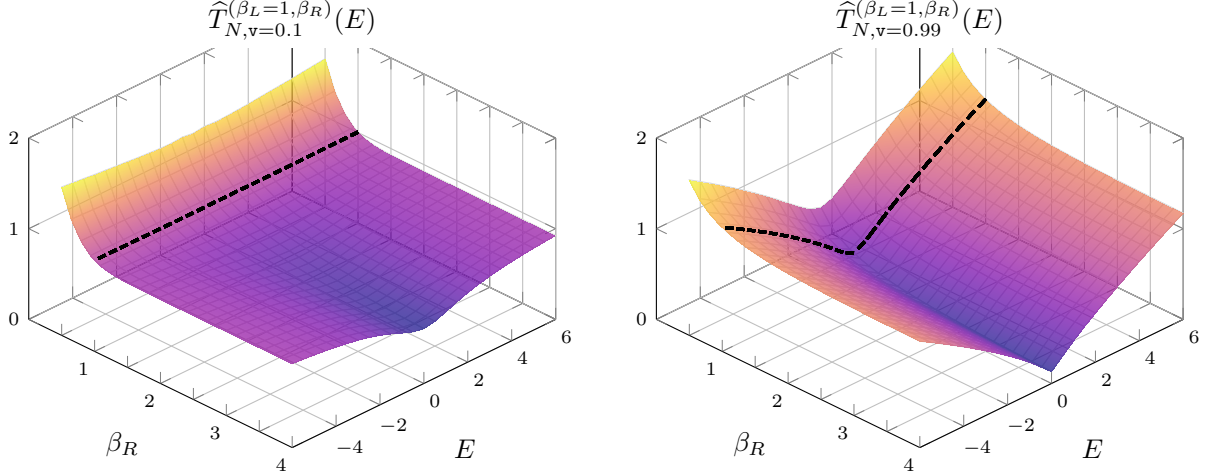


Figure 8: Plot of the effective temperature $\widehat{T}_{N,v}^{(\beta_L, \beta_R)}$ for $\beta_L = 1$, and $\beta_R = 10$ (top panel) and $\beta_R = 0.1$ (bottom panel), for different values of v as indicated in the legend. The zero velocity limit $\widehat{T}_{N,0}^{(\beta_L, \beta_R)}$ is shown by the solid gray curves.

Figure 8 shows the dependence of $\widehat{T}_{N,v}^{(\beta_L, \beta_R)}$ on v and the KMS parameters of the semi-infinite heat baths in a neighborhood of $E = 0$. For concreteness, we have chosen $\beta_L = 1$ and $\beta_R \in \{0.1, 10\}$. One observes that for fixed KMS parameters the effective temperature may be



(a) $(\beta_R, E) \mapsto \widehat{T}_{N,\mathbf{v}=0.1}^{(\beta_L=1,\beta_R)}(E)$ ($\beta_R > 0.5$)

(b) $(\beta_R, E) \mapsto \widehat{T}_{N,\mathbf{v}=0.99}^{(\beta_L=1,\beta_R)}(E)$ ($\beta_R > 0.5$)

Figure 9: Surface plots of the effective temperature $(\beta_R, E) \mapsto \widehat{T}_{N,\mathbf{v}}^{(\beta_L,\beta_R)}(E)$ for $\beta_L = 1$, $\beta_R > 0.5$, and $\mathbf{v} = 0.1$ (left), 0.99 (right). The dashed surface curves at $\beta_R = \beta_L = 1$ correspond to $E \mapsto \widehat{T}_{\mathbf{v}}^{(1)}(E)$ given by Eq. (4.1) (as a consequence of $\mathcal{R}_{N,\mathbf{v}}^{(\beta,\beta)} = \mathcal{R}_{\mathbf{v}}^{(\beta)}$).

higher or lower than $\widehat{T}_{N,0}^{(\beta_L,\beta_R)}$ (the solid gray curves in the figure) for certain velocities, and it is not an even function of \mathbf{v} . Moreover, the relationship between the effective temperatures at different velocities changes depending on the KMS parameters, more specifically on whether β_R is higher or lower than β_L . We see that the effective temperature $\widehat{T}_{N,\mathbf{v}}^{(\beta_L,\beta_R)}$ near $E = 0$ exceeds $\widehat{T}_{N,0}^{(\beta_L,\beta_R)}$ when the detector moves against the direction of the heat flow, except for $|\mathbf{v}| = 0.99$ near the speed of light. (Recall from Eq. (3.1) that the detector moves from left to right towards $x^1 = +\infty$ for $\mathbf{v} > 0$, and reverse for $\mathbf{v} < 0$.) Figure 9 illustrates the dependence of $\widehat{T}_{N,\mathbf{v}}^{(\beta_L,\beta_R)}$ on β_R in a surface plot for $\beta_L = 1$ and arbitrarily chosen velocities $\mathbf{v} \in \{0.1, 0.99\}$. The limit $\beta_R \rightarrow \infty$ is given by

$$\widehat{T}_{N,\mathbf{v}}^{(\beta_L,\infty)}(E) = \frac{|E|}{\ln\left(1 + \frac{|E|}{2\pi R(\beta_L,\mathbf{v},|E|)}\right)}$$

for the function R defined in Eq. (3.16) and $\beta_L > 0$, $\mathbf{v} \in (-1, 1) \setminus \{0\}$, $E \in \mathbb{R} \setminus \{0\}$. Its properties will not be studied here.

Expanded in E it holds (see Eq. (3.17))

$$\widehat{T}_{N,\mathbf{v}}^{(\beta_L,\beta_R)}(E) = \frac{\sqrt{1-\mathbf{v}^2}}{2\mathbf{v}} \left(\frac{1}{\beta_L} \ln(1+\mathbf{v}) - \frac{1}{\beta_R} \ln(1-\mathbf{v}) \right) + \mathcal{O}(E^2).$$

Compared to (KMS- \mathbf{v}) (Eq. (4.1)), the behavior of $\widehat{T}_{N,\mathbf{v}}^{(\beta_L,\beta_R)}(E)$ in \mathbf{v} for small $|E|$ is similar to the transition rates shown in the left plot of Figure 3: Unless $\beta_L = \beta_R$, there is an asymmetry in \mathbf{v} and a maximum value of $\widehat{T}_{N,\mathbf{v}}^{(\beta_L,\beta_R)}(E)$ for some $|\mathbf{v}| > 0$ depending on $\text{sgn}(\beta_L - \beta_R)$. For

slowly moving detectors sensitive to the infrared regime,

$$\widehat{T}_{N,\mathbf{v}}^{(\beta_L,\beta_R)}(E) \simeq \frac{1}{2}(\beta_L^{-1} + \beta_R^{-1}) + \frac{\beta_L - \beta_R}{4\beta_L\beta_R}\mathbf{v} - \frac{\beta_L + \beta_R}{12\beta_L\beta_R}\mathbf{v}^2, \quad |\mathbf{v}| \ll 1, E \rightarrow 0. \quad (4.5)$$

Under the same conditions, $\widehat{T}_{\mathbf{v}}^{(\beta)}$ given in Eq. (4.2) is strictly smaller than the corresponding rest frame temperature β^{-1} . By contrast, the right-hand side of Eq. (4.5) is larger than $\lim_{E \rightarrow 0} \widehat{T}_{N,0}^{(\beta_L,\beta_R)}(E) = \frac{1}{2}(\beta_L^{-1} + \beta_R^{-1})$ (Eq. (4.3)) for positive (negative) \mathbf{v} with $|\mathbf{v}| \ll 1$ when $\beta_L > \beta_R$ ($\beta_L < \beta_R$).

5. The comoving frame

In this section we introduce the comoving frame of the NESS as a proposal for a reference frame that comes closest to the rest frame of a thermal equilibrium state and thus could be a suitable frame for the comparison of detector responses in future investigations.

For $\beta_R > \beta_L > 0$ there is a heat flow from $x^1 = -\infty$ to $x^1 = \infty$ in the NESS described by ω_N (and in the reverse direction for $0 < \beta_R < \beta_L$) [DLSB15, HV18]. The idea is to consider the special case of (NESS- \mathbf{v}) in which the detector couples to the NESS in a reference frame where the heat flow is “at rest”, i.e. the detector moves with the heat flow at a certain constant velocity that depends on β_L, β_R . This frame is characterized by the property that the expected stress-energy tensor of the field is diagonalized, in analogy to the (local) rest frame of a perfect fluid (which is fully described by a non-zero energy density and isotropic pressure [Sch09]). The heat flow is thereby rendered as a velocity effect that is compensated kinematically by boosting to the comoving rest frame of the flow. A stationary detector in this frame is at rest relative to the “medium” of the NESS, similar to the thermal case (KMS-0). We argue that the detector behavior should be studied relative to this frame, in the spirit of the (widely supported) guiding principle that thermal properties of systems ought to be determined by distinguished quantities defined relative to their rest frame; see, e.g., [CS69, CH71, CM95b, LM96, LM04, Sew08, Sew09, Sew10, PV25]. This also constitutes a fundamental premise for the definition of local thermal equilibrium states of quantum fields [BOR02].

The stress-energy tensor of the massless scalar field ϕ is given by (see, e.g., [BD82])

$$T_{\mu\nu} = : \partial_\mu \phi \partial_\nu \phi - \frac{1}{2} \eta_{\mu\nu} \partial_\rho \phi \partial^\rho \phi : , \quad (5.1)$$

where η is the Minkowski metric tensor, the colons denote normal ordering with respect to the vacuum state, and Einstein’s summation convention is implied. Using Eq. (2.10) we show in Lemma D.1 (rederiving results from [DLSB15]) that the expected stress-energy tensor of

the NESS ω_N (constructed in the inertial frame I) has block diagonal form, namely

$$(\mathcal{T}_{\mu\nu}) := (\omega_N(T_{\mu\nu})) = \begin{pmatrix} \tilde{\mathcal{T}} & 0_2 \\ 0_2 & \text{diag}(\mathcal{T}_\perp, \mathcal{T}_\perp) \end{pmatrix}, \quad (5.2)$$

where 0_2 is the 2×2 zero matrix, and

$$\tilde{\mathcal{T}} = \begin{pmatrix} \mathcal{T}_{00} & \mathcal{T}_{01} \\ \mathcal{T}_{01} & \mathcal{T}_{11} \end{pmatrix}, \quad \mathcal{T}_\perp := \mathcal{T}_{22} = \mathcal{T}_{33}$$

for non-zero expected energy current density \mathcal{T}_{01} [DLSB15] (see Lemma D.2).

Proposition 5.1

Let $\beta_L, \beta_R > 0$, $\beta_L \neq \beta_R$. There exists a Lorentz boost Λ_N in the x^1 -direction that diagonalizes the expected stress-energy tensor of the NESS ω_N , i.e. $(\Lambda_N)_\mu{}^\rho (\Lambda_N)_\nu{}^\sigma \mathcal{T}_{\rho\sigma} = 0$ for all $\mu \neq \nu$. The corresponding velocity $\mathbf{v}_N(\beta_L, \beta_R)$ of the boost (as active transformation of the frame I) is given by

$$\mathbf{v}_N(\beta_L, \beta_R) = \kappa(\beta_L, \beta_R) - \text{sgn}(\beta_R - \beta_L) \sqrt{\kappa(\beta_L, \beta_R)^2 - 1}, \quad \kappa(\beta_L, \beta_R) := \frac{4}{3} \frac{\beta_R^4 + \beta_L^4}{\beta_R^4 - \beta_L^4},$$

which can be written as

$$\mathbf{v}_N(\beta_L, \beta_R) = \frac{4(\beta_R^4 + \beta_L^4) - \sqrt{(\beta_R^4 + 7\beta_L^4)(\beta_L^4 + 7\beta_R^4)}}{3(\beta_R^4 - \beta_L^4)}$$

and satisfies the bound $|\mathbf{v}_N(\beta_L, \beta_R)| < \frac{4-\sqrt{7}}{3} \approx 0.4514$. Under the boost Λ_N the diagonalized expected stress-energy tensor is not isotropic, i.e. its (11) and (22) components are distinct.

The reference frame obtained from I under the boost Λ_N is called the *comoving frame*.

Proof.

Let Λ be a Lorentz boost in x^1 -direction given (as active transformation) by

$$\Lambda = \begin{pmatrix} \tilde{\Lambda} & 0_2 \\ 0_2 & \mathbb{1}_2 \end{pmatrix}, \quad \tilde{\Lambda} = \begin{pmatrix} \gamma & \gamma \mathbf{v} \\ \gamma \mathbf{v} & \gamma \end{pmatrix}, \quad (5.3)$$

where $\mathbb{1}_2$ is the 2×2 unit matrix, and $\mathbf{v} \in (-1, 1)$. It holds $\Lambda_\mu{}^\rho \Lambda_\nu{}^\sigma \mathcal{T}_{\rho\sigma} = 0$ for all $\mu \neq \nu$ if and only if $\Lambda^{-1}(\mathcal{T}_{\mu\nu})\Lambda^{-1}$ is a diagonal matrix. This is the case when $\tilde{\Lambda}^{-1}\tilde{\mathcal{T}}\tilde{\Lambda}^{-1}$ is a diagonal 2×2 matrix. A straightforward calculation shows that

$$\tilde{\Lambda}^{-1}\tilde{\mathcal{T}}\tilde{\Lambda}^{-1} = \gamma^2 \begin{pmatrix} \mathcal{T}_{00} - 2\mathcal{T}_{01}\mathbf{v} + \mathcal{T}_{11}\mathbf{v}^2 & -(\mathcal{T}_{00} + \mathcal{T}_{11})\mathbf{v} + \mathcal{T}_{01}(1 + \mathbf{v}^2) \\ -(\mathcal{T}_{00} + \mathcal{T}_{11})\mathbf{v} + \mathcal{T}_{01}(1 + \mathbf{v}^2) & \mathcal{T}_{11} - 2\mathcal{T}_{01}\mathbf{v} + \mathcal{T}_{00}\mathbf{v}^2 \end{pmatrix}, \quad (5.4)$$

whose off-diagonal component vanishes for \mathbf{v} satisfying $\mathbf{v}^2 - (\mathcal{T}_{00} + \mathcal{T}_{11})\mathbf{v}/\mathcal{T}_{01} + 1 = 0$. The

solutions are

$$\mathbf{v}_\pm = \frac{\mathcal{T}_{00} + \mathcal{T}_{11}}{2\mathcal{T}_{01}} \pm \sqrt{\left(\frac{\mathcal{T}_{00} + \mathcal{T}_{11}}{2\mathcal{T}_{01}}\right)^2 - 1}$$

under the condition $\mathbf{v}_\pm \in (-1, 1)$, which is satisfied by one of the solutions for any $\beta_L, \beta_R > 0$, $\beta_L \neq \beta_R$. In Lemma D.2 we verify that

$$\frac{\mathcal{T}_{00} + \mathcal{T}_{11}}{2\mathcal{T}_{01}} = \frac{4}{3} \frac{\beta_R^4 + \beta_L^4}{\beta_R^4 - \beta_L^4} =: \kappa(\beta_L, \beta_R).$$

Clearly, $|\kappa(\beta_L, \beta_R)| > \frac{4}{3}$ for all $\beta_L, \beta_R > 0$, $\beta_L \neq \beta_R$. We have $\kappa(\beta_L, \beta_R) > \frac{4}{3}$ (respectively, $\kappa(\beta_L, \beta_R) < -\frac{4}{3}$) if and only if $\beta_R > \beta_L > 0$ (respectively, $0 < \beta_R < \beta_L$), in which case the unique velocity of the Lorentz boost diagonalizing the expected stress-energy tensor is $\mathbf{v}_- \in (0, \frac{4-\sqrt{7}}{3})$ (respectively, $\mathbf{v}_+ \in (-\frac{4-\sqrt{7}}{3}, 0)$). Combining these two cases yields the velocity $\mathbf{v}_N(\beta_L, \beta_R)$ as stated.

Considering a general Lorentz boost Λ with velocity \mathbf{v} in x^1 -direction as in Eq. (5.3), the (11) component of $\Lambda^{-1}(\mathcal{T}_{\mu\nu})\Lambda^{-1}$ is given by $\gamma^2(\mathcal{T}_{11} - 2\mathcal{T}_{01}\mathbf{v} + \mathcal{T}_{00}\mathbf{v}^2)$ by Eq. (5.4), whereas the (22) component (which is the same as the (33) component) equals $\frac{1}{3}\mathcal{T}_{00}$ by Lemma D.2. Using that $\mathcal{T}_{11} = \frac{1}{3}\mathcal{T}_{00}$ (see again Lemma D.2), one finds that the (11) and (22) components of $\Lambda^{-1}(\mathcal{T}_{\mu\nu})\Lambda^{-1}$ coincide either when $\mathbf{v} = 0$ (which we can dismiss, because $\mathbf{v}_N(\beta_L, \beta_R) \neq 0$ for $\beta_L \neq \beta_R$), or

$$\mathbf{v} = \frac{3\mathcal{T}_{01}}{2\mathcal{T}_{00}} = \frac{3}{4} \frac{\beta_R^4 - \beta_L^4}{\beta_R^4 + \beta_L^4} \equiv \frac{1}{\kappa(\beta_L, \beta_R)}.$$

Since $|\mathbf{v}_N(\beta_L, \beta_R)| < |\kappa(\beta_L, \beta_R)^{-1}|$ for all $\beta_L, \beta_R > 0$, $\beta_L \neq \beta_R$, the (11) and (22) components of the expected stress-energy tensor in the comoving frame do not coincide. \square

Some remarks on the velocity of the comoving frame are in order. It is antisymmetric in the initial KMS parameters β_L, β_R of the NESS, i.e. $\mathbf{v}_N(\beta_L, \beta_R) = -\mathbf{v}_N(\beta_R, \beta_L)$. This reflects the physical picture that the direction of the heat flow is reversed when the thermal reservoirs are swapped. The bound $|\mathbf{v}_N(\beta_L, \beta_R)| < \frac{4-\sqrt{7}}{3}$ is an interesting property that is a consequence of the expectation value of the stress-energy tensor in four spacetime dimensions (see Appendix D). If one of the semi-infinite heat baths is prepared in the vacuum state, i.e. $\beta_L > 0$ and $\beta_R \rightarrow \infty$ or vice versa, we have $|\kappa(\beta_L, \beta_R)| \rightarrow \frac{4}{3}$ and thus $|\mathbf{v}_N(\beta_L, \beta_R)| \rightarrow \frac{4-\sqrt{7}}{3} \approx 0.4514$. Similarly, $|\mathbf{v}_N(\beta_L, \beta_R)| \rightarrow \frac{4-\sqrt{7}}{3}$ when one of the reservoirs approaches infinitely high temperature, $\beta_{L/R} \rightarrow 0$. Hence the heat flow of the NESS always travels subluminally (see Figure 10a).

This is in contrast to the NESS σ_N of the massless scalar field on two-dimensional Minkowski spacetime, for which $\sigma_N(T_{00}) = \sigma_N(T_{11}) = \frac{\pi}{12}(\beta_L^{-2} + \beta_R^{-2})$ and $\sigma_N(T_{01}) = \sigma_N(T_{10}) = \frac{\pi}{12}(\beta_L^{-2} - \beta_R^{-2})$ (see [DLSB15]). The velocity of the boost that diagonalizes the expected stress-energy

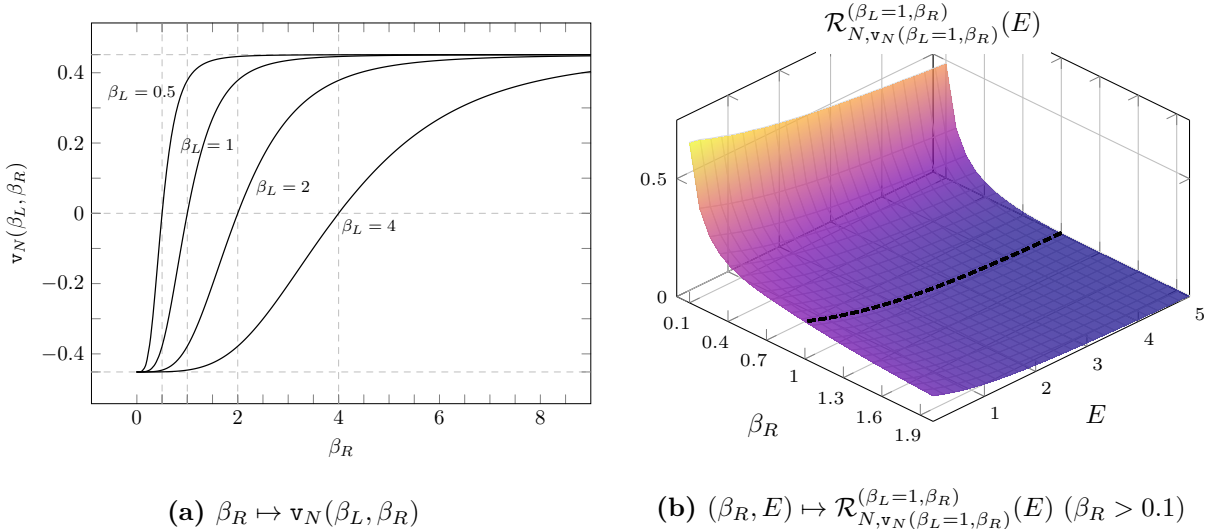


Figure 10: (a) Plot of the velocity $v_N(\beta_L, \beta_R)$ of the comoving frame as a function of β_R for different fixed values of β_L . The velocity $v_N(\beta_L, \beta_R)$ is negative when $\beta_R < \beta_L$, and positive when $\beta_R > \beta_L$. The modulus of the velocity is bounded by $\frac{4-\sqrt{7}}{3} \approx 0.4514$. The velocity function v_N extends to (β_L, β_R) with $\beta_R = \beta_L$, where it vanishes. The functions $\beta_L \mapsto v_N(\beta_L, \beta_R)$ for fixed β_R are obtained via reflection along the horizontal axis. (b) Surface plot of $(\beta_R, E) \mapsto \mathcal{R}_{N, v_N(\beta_L=1, \beta_R)}^{(\beta_L=1, \beta_R)}(E)$ for $v = v_N(\beta_L, \beta_R)$, $\beta_L = 1$, and $\beta_R > 0.1$, $E > 0$. The dashed surface curve at $\beta_R = 1$ (in which case the detector interacts with a $(\beta = 1)$ -KMS state and $v_N \rightarrow 0$) represents the Planckian $\mathcal{R}_0^{(\beta=1)}$.

tensor in that case is given by

$$\mathbf{v}_1 := \kappa_1 - \text{sgn}(\beta_R - \beta_L) \sqrt{\kappa_1^2 - 1} = \frac{\beta_R - \beta_L}{\beta_R + \beta_L}, \quad \kappa_1 := \frac{\sigma_N(T_{00})}{\sigma_N(T_{01})} = \frac{\beta_R^2 + \beta_L^2}{\beta_R^2 - \beta_L^2},$$

which is precisely the boost velocity for the frame in which σ_N is a KMS state of temperature $(\beta_L \beta_R)^{-1/2}$ [DLSB15] (see also [BDLS15]). The modulus of \mathbf{v}_1 approaches the speed of light in the ground state limit of one of the heat baths.

As noted at the beginning of this section, we propose that the significance of the comoving frame for the study of detectors coupled to NESS arises from the paradigm that the instantaneous rest frame of a system is the preferred reference frame for the formulation of its thermal properties. For the NESS with initial heat bath KMS parameters β_L, β_R the comoving frame with velocity $v_N(\beta_L, \beta_R)$ is the inertial rest frame of the heat flow of the NESS. In the case (NESS- v_N) in which the detector moves along the x^1 -axis with velocity $v_N(\beta_L, \beta_R)$ relative to the inertial frame I , the transition rate is given by $\mathcal{R}_{N, v_N(\beta_L, \beta_R)}^{(\beta_L, \beta_R)}$ (Eq. (3.15)), which is now a function of β_L, β_R, E . The transition rate $\mathcal{R}_{N, v_N(\beta_L, \beta_R)}^{(\beta_L, \beta_R)}$ is kept invariant when the KMS parameters β_L, β_R are swapped, thanks to the property $v_N(\beta_L, \beta_R) = -v_N(\beta_R, \beta_L)$ (cf. the discussion below Eq. (3.17)). The heat flow is absent and the relative velocity of the comoving frame vanishes when $\beta_L = \beta_R =: \beta$ (see Figure 10a), so the transition rate $\mathcal{R}_{N, v_N(\beta_L, \beta_R)}^{(\beta_L, \beta_R)}$ of the detector reduces to $\mathcal{R}_0^{(\beta)}$, the Planckian transition rate of the detector at rest relative to the KMS state (see Eqs. (3.15) & (3.6)). In a sense, choosing the relative velocity \mathbf{v} of the

detector to be the temperature-dependent velocity \mathbf{v}_N provides an interpolation between the transition rates of the cases (NESS- \mathbf{v}) and (KMS-0) as the parameters β_L, β_R are varied.

Figure 10b shows a plot of $(\beta_R, E) \mapsto \mathcal{R}_{N, \mathbf{v}_N(1, \beta_R)}^{(1, \beta_R)}(E)$ for $E > 0$. Although the detector is at rest relative to the heat flow (the “medium” of the NESS), the response is non-thermal (unless $\beta_L = \beta_R$), thus showing a difference to the case of a detector that couples to the rest frame of an inertial heat bath. This is in line with the anisotropy of the expected stress-energy tensor in the comoving frame (Proposition 5.1): While the transformation to the comoving frame compensates the impact of the heat flow in longitudinal direction (so the expected stress-energy tensor is diagonalized), transversal modes still transmit (Doppler shifted) energy and momentum to the detector under the isotropic monopole coupling. Further studies of the response with other detector couplings could reveal more details regarding this behavior.

6. Conclusions and outlook

In this work we studied the transition rate of a two-level Unruh-DeWitt detector that is coupled via a point-like monopole interaction to the NESS of a free massless scalar field as constructed in [HV18]. The latter arises from bringing two semi-infinite heat baths, described by inertial KMS states at inverse temperatures $\beta_L, \beta_R > 0$, into contact in a neighborhood of the hypersurface $\{x \in \mathbb{M} : x^1 = 0\}$. If the detector is at rest relative to the defining inertial (laboratory) frame of the NESS (Section 3.2), the transition rate equals the arithmetic mean of the Planckian rates associated to the two heat baths. The NESS looks to the detector like a mixture of KMS states and thus the response corresponds to an interaction with a state that is passive [PW78, FV03] (see also [FV15, Sec. 4.8.2]) but not in thermal equilibrium at some uniquely assigned temperature. For non-zero constant velocity along the x^1 -axis (Section 3.3) the form of the detector’s transition rate can be traced back to purely kinematical effects (Doppler effect). This is structurally similar to the response obtained from the motion relative to a thermal bath [CM95a, CM95b, LM96], reviewed in Section 3.1. As a special case we considered the limit $\beta_R \rightarrow \infty$ that brings the right reservoir into the vacuum state, and discussed the dependence of the corresponding transition rate on the relative velocity of the detector. In particular, a low velocity expansion allowed to highlight differences to the case of a detector moving in a heat bath [Cos04]. In Section 4 we collected some properties of the corresponding effective temperatures obtained from the detailed balance condition. These results may represent a starting point for further research of NESS being probed by Unruh-DeWitt detectors, as there are several topics we have not pursued here (e.g., numerical analysis of transition rates and effective temperatures; ramifications with regards to the comoving inertial frame that moves with the heat flow of the NESS; influence of other detector couplings, spacetime dimensions, and non-zero mass parameter of the field).

The main takeaway from our results is that a monopole detector coupled to a NESS is, in general, not sensitive to dynamical features. A proper “NESS detector” should be able to

pick up the current of the heat flow and convert its energy-momentum into internal energy, which then would be visible in the transition rate already for a detector at rest. In case such a detector moves along with the heat flow by being at rest relative to the comoving frame (as introduced in Section 5), one would expect that the response corresponds to a passive state, since in this frame the current is compensated and thus one cannot extract energy from it via cyclic processes. (To try the analogy employed in [BS13], the detector is stationary in the rest frame of the spinning “pinwheel”, characterized by zero flow velocity from the detector’s perspective.) All of this certainly depends on the choice of detector model and detector-field interaction. Couplings of interest could involve higher moment operators; see, e.g., [Hin83, Mou18, PA20, Tak86, MA98] (and references therein) for some works that consider dipole moments in the interaction with a derivative of a scalar field or in the context of model atoms coupled to an electromagnetic field. More specifically, a dynamical coupling to the heat flow might be achieved by means of a dipole (or multipole) moment that couples to tensorial, current-related quantities of the NESS, like the stress-energy tensor (see [PS87] for such a model). This could facilitate the study of (an)isotropy of the heat flow of the NESS from the perspective of the detector.

Finally, our discussion reflects the well-known subtlety of the concept of temperature in non-equilibrium and relativistic systems [CJ03, Neu80]. In certain instances it might be sensible to assign an effective temperature to a relativistic NESS. For example, one can introduce a Lorentz-invariant “proper effective temperature” based on gauge-gravity duality [HN20] (see also references therein). However, the non-Planckian transition rates in Sections 3.2 & 3.3 and the corresponding (energy-dependent) detailed balance temperatures obtained in Section 4 reveal that generally such a quantity will not be a temperature by way of Unruh-DeWitt detectors, i.e. it is not a temperature from a microscopic (Boltzmann-Gibbs) viewpoint (cf. [Haa96]). As far as the response of the detector is concerned, the NESS does not have a uniquely determined temperature, similar to heat baths from the perspective of moving inertial reference frames [CM95b, LM96, LM04]. The mentioned limitation of the detector setup to measure dynamical properties of the NESS motivates a deeper investigation of these topics.

Acknowledgments The authors thank Marco Merkli for discussion and pointing out several references regarding NESS. A.G.P. is indebted to the IMPRS and MPI for Mathematics in the Sciences, Leipzig, where early parts of this work have been conceived, for support and hospitality. R.V. gratefully acknowledges funding by the CY Initiative of Excellence (grant “Investissements d’Avenir” ANR-16-IDEX-0008) during his stay at the CY Advanced Studies.

A. Transition rate of detector moving through heat bath

In this appendix we prove Eq. (3.4), the transition rate of an Unruh-DeWitt monopole detector moving with constant non-zero velocity while coupled to a four-dimensional massless scalar field at positive temperature. The result has been stated before by Costa & Matsas [CM95a, CM95b]. (For a detector coupled to the time derivative of a scalar field on three-dimensional Minkowski spacetime a corresponding result can be found in [BL23].) Serving as reference in the main text, we present a derivation starting from the two-point function W_β of the field's β -KMS state ω_β ($\beta > 0$) given by Eq. (2.7).

By the Hadamard property, $\widetilde{W}_\beta := W_\beta - W_{\text{vac}}$ (for the vacuum two-point function W_{vac} , see Eqs. (2.5) & (2.6)) is a smooth function on $\mathbb{M} \times \mathbb{M}$. It can be written in the form (see [Wel00] and [FZ11, Sec. F.3.5])

$$\begin{aligned} \widetilde{W}_\beta(x, y) &= \frac{1}{4\pi^2 \left((x^0 - y^0)^2 - \|\underline{x} - \underline{y}\|^2 \right)} + \\ &+ \frac{1}{8\pi\beta\|\underline{x} - \underline{y}\|} \left[\coth \left(\frac{\pi}{\beta} (x^0 - y^0 + \|\underline{x} - \underline{y}\|) \right) - \coth \left(\frac{\pi}{\beta} (x^0 - y^0 - \|\underline{x} - \underline{y}\|) \right) \right]. \end{aligned} \quad (\text{A.1})$$

For the sake of self-containment, let us derive this expression from the distributional integral representations of W_{vac} and W_β . As these two-point functions only depend on $x - y$ we can set $y = 0$ without loss of generality. Using spherical coordinates,

$$\begin{aligned} \widetilde{W}_\beta(x, 0) &= \frac{1}{(2\pi)^3} \int_{\mathbb{R}^3} \frac{1}{2\|\underline{p}\|} \left(\frac{e^{i\|\underline{p}\|x^0} e^{-i\underline{p} \cdot \underline{x}}}{e^{\beta\|\underline{p}\|} - 1} - e^{-i\|\underline{p}\|x^0} e^{i\underline{p} \cdot \underline{x}} \left(\frac{1}{e^{-\beta\|\underline{p}\|} - 1} + 1 \right) \right) d^3 \underline{p} = \\ &= \frac{1}{(2\pi)^3} \int_{\mathbb{R}^3} \frac{1}{2\|\underline{p}\|} \frac{e^{i\|\underline{p}\|x^0} e^{-i\underline{p} \cdot \underline{x}} + e^{-i\|\underline{p}\|x^0} e^{i\underline{p} \cdot \underline{x}}}{e^{\beta\|\underline{p}\|} - 1} d^3 \underline{p} = \frac{1}{(2\pi)^3} \int_{\mathbb{R}^3} \frac{1}{\|\underline{p}\|} \frac{\cos(\|\underline{p}\|x^0 - \underline{p} \cdot \underline{x})}{e^{\beta\|\underline{p}\|} - 1} d^3 \underline{p} = \\ &= \frac{1}{(2\pi)^2} \int_0^\infty \int_0^\pi \frac{r \cos(rx^0 - r\|\underline{x}\| \cos(\theta))}{e^{\beta r} - 1} \sin(\theta) d\theta dr. \end{aligned} \quad (\text{A.2})$$

If $\underline{x} = \underline{0}$,

$$\widetilde{W}_\beta(x, 0) = \frac{1}{2\pi^2} \int_0^\infty \frac{r \cos(rx^0)}{e^{\beta r} - 1} dr = \frac{1}{4\pi^2(x^0)^2} - \frac{1}{4\beta^2} \frac{1}{\sinh^2\left(\frac{\pi}{\beta}x^0\right)} \quad (\text{A.3})$$

by [EMOT54, Sec. 1.4, (8)] (employing symmetry for the case $x^0 < 0$). For $x^0 = 0$ the integral equals $\int_0^\infty r(e^{\beta r} - 1)^{-1} dr = \frac{\pi^2}{6\beta^2}$ (see [EMOT54, Sec. 6.3, (7)]) and thus $\widetilde{W}_\beta(0, 0) = \frac{1}{12\beta^2} = \widetilde{W}_\beta(x, x)$ (for all $x \in \mathbb{M}$), which coincides with the limit of the right-hand side of Eq. (A.3) as $x^0 \rightarrow 0$. If $\underline{x} \neq \underline{0}$, then Eq. (A.2) yields

$$\widetilde{W}_\beta(x, 0) = \frac{1}{2\pi^2\|\underline{x}\|} \int_0^\infty \frac{\cos(rx^0) \sin(r\|\underline{x}\|)}{e^{\beta r} - 1} dr = \frac{1}{4\pi^2\|\underline{x}\|} \sum_{\varsigma=\pm 1} \varsigma \int_0^\infty \frac{\sin(r(x^0 + \varsigma\|\underline{x}\|))}{e^{\beta r} - 1} dr$$

by the usual trigonometric identity for the product of sine and cosine. The resulting integral is a Fourier sine transform given in [EMOT54, Sec. 2.4, (11)]:

$$\int_0^\infty \frac{\sin(qr)}{e^{\beta r} - 1} dr = -\frac{1}{2q} + \frac{\pi}{2\beta} \coth\left(\frac{\pi q}{\beta}\right), \quad \beta, q > 0 \quad (\text{A.4})$$

This can be shown using $(e^{\beta r} - 1)^{-1} = \sum_{n=1}^\infty e^{-n\beta r}$ and the series expansion $\coth(\pi x) = \frac{1}{\pi x} + \frac{2x}{\pi} \sum_{n=1}^\infty (n^2 + x^2)^{-1}$, $x \neq 0$ [DLMF, 4.36.3]. Eq. (A.4) also applies to $q < 0$ by symmetry, and the right-hand side extends smoothly to zero as $q \rightarrow 0$, which allows to interpret the expression as said extension to $q \in \mathbb{R}$. Hence

$$\widetilde{W}_\beta(x, 0) = \frac{1}{4\pi^2 \|\underline{x}\|} \sum_{\varsigma=\pm 1} \varsigma \left(-\frac{1}{2(x^0 + \varsigma \|\underline{x}\|)} + \frac{\pi}{2\beta} \coth\left(\frac{\pi}{\beta} (x^0 + \varsigma \|\underline{x}\|)\right) \right),$$

which extends smoothly to all $x \in \mathbb{M}$ and results in Eq. (A.1) after reinstating y by $\widetilde{W}_\beta(x, y) = \widetilde{W}_\beta(x - y, 0)$.

Now let $\widetilde{w}_{\beta, \mathbf{v}}(s) := \widetilde{W}_\beta(\mathbf{x}_\mathbf{v}(s), 0) \equiv (W_\beta - W_{\text{vac}})(\mathbf{x}_\mathbf{v}(s), 0)$ for the inertial detector worldline $\tau \mapsto \mathbf{x}_\mathbf{v}(\tau) = \gamma(\tau, \mathbf{v}\tau, 0, 0)$ with $0 < |\mathbf{v}| < 1$. Using Eq. (A.1) one finds that

$$\begin{aligned} \widetilde{w}_{\beta, \mathbf{v}}(s) &= \frac{1}{4\pi^2 s^2} + \frac{1}{8\pi\beta\gamma|\mathbf{v}s|} \left(\coth\left(\frac{\pi\gamma}{\beta}(s + |\mathbf{v}s|)\right) - \coth\left(\frac{\pi\gamma}{\beta}(s - |\mathbf{v}s|)\right) \right) = \\ &= \frac{1}{4\pi^2 s^2} + \frac{1}{8\pi\beta\gamma\mathbf{v}s} \left(\coth\left(\frac{\pi s}{\beta\mathbf{d}_-}\right) - \coth\left(\frac{\pi s}{\beta\mathbf{d}_+}\right) \right) = \\ &= \frac{1}{4\pi\beta\gamma\mathbf{v}} \left[\frac{\beta\gamma\mathbf{v}}{\pi s^2} + \frac{1}{2s} \coth\left(\frac{\pi s}{\beta\mathbf{d}_-}\right) - \frac{1}{2s} \coth\left(\frac{\pi s}{\beta\mathbf{d}_+}\right) \right], \end{aligned}$$

where \mathbf{d}_\pm are the Doppler factors defined in Eq. (3.2). The transition rate (Eq. (2.4)) in question is

$$\mathcal{R}_\mathbf{v}^{(\beta)}(E) = \int_{\mathbb{R}} e^{-iEs} \widetilde{w}_{\beta, \mathbf{v}}(s) ds - \frac{E}{2\pi} \Theta(-E) \quad (\text{A.5})$$

for $E \in \mathbb{R} \setminus \{0\}$, where we split off the vacuum contribution that is given by Eq. (3.3). To prove Eq. (3.4) we show that

$$\int_{\mathbb{R}} e^{-iEs} \widetilde{w}_{\beta, \mathbf{v}}(s) ds = \frac{1}{4\pi\beta\gamma\mathbf{v}} \ln\left(\frac{1 - e^{-\beta\mathbf{d}_+|E|}}{1 - e^{-\beta\mathbf{d}_-|E|}}\right). \quad (\text{A.6})$$

First, we write $\gamma\mathbf{v} = \frac{1}{2}(\mathbf{d}_+ - \mathbf{d}_-)$ to obtain

$$\widetilde{w}_{\beta, \mathbf{v}}(s) = \frac{1}{4\pi\beta\gamma\mathbf{v}} (f_{\beta\mathbf{d}_+}(s) - f_{\beta\mathbf{d}_-}(s)), \quad (\text{A.7})$$

$$f_c(s) := \frac{c}{2\pi s^2} - \frac{1}{2s} \coth\left(\frac{\pi s}{c}\right) = -\frac{c}{\pi} \sum_{n=1}^{\infty} \frac{1}{n^2 c^2 + s^2}, \quad c > 0. \quad (\text{A.8})$$

Note that the Laurent series expansion of $s \mapsto \frac{1}{2s} \coth\left(\frac{\pi s}{c}\right)$ in a punctured neighborhood of $s = 0$ has the singular part $\frac{c}{2\pi s^2}$, and $\lim_{s \rightarrow 0} f_c(s) = -\frac{\pi}{6c}$. For every $c > 0$, the function f_c is interpreted as the unique extension of the given expression to an analytic function on \mathbb{R} as signified by the stated series expansion in Eq. (A.8) (see [DLMF, 4.36.3]). The Fourier cosine transform $\int_0^\infty \cos(sx) \ln(1 - e^{-cx}) dx = \pi f_c(s)$ (for $c, s > 0$) from [EMOT54, Sec. 1.5, (14)] can be inverted to $\int_0^\infty \cos(qs) f_c(s) ds = \frac{1}{2} \ln(1 - e^{-cq})$ for $c, q > 0$. One can verify this explicitly by using the series expansion of f_c and $\int_0^\infty \cos(qs) (n^2 c^2 + s^2)^{-1} ds = \frac{\pi}{2nc} e^{-ncq}$ for $c, q > 0$ and integers $n \geq 1$ [EMOT54, Sec. 1.2, (11)]. Since f_c is an even function for every $c > 0$, the sine part of its Fourier transform vanishes and one obtains

$$\int_{\mathbb{R}} e^{-iEs} f_c(s) ds = 2 \int_0^\infty \cos(|E|s) f_c(s) ds = \ln(1 - e^{-c|E|}). \quad (\text{A.9})$$

Combining Eqs. (A.7) & (A.9) implies Eq. (A.6). For $E < 0$,

$$\begin{aligned} \int_{\mathbb{R}} e^{-iEs} \tilde{w}_{\beta, \mathbf{v}}(s) ds &= \frac{1}{4\pi\beta\gamma\mathbf{v}} \ln\left(\frac{1 - e^{\beta\mathbf{d}_+ E}}{1 - e^{\beta\mathbf{d}_- E}}\right) = \frac{1}{4\pi\beta\gamma\mathbf{v}} \ln\left(e^{\beta(\mathbf{d}_+ - \mathbf{d}_-)E} \frac{e^{-\beta\mathbf{d}_+ E} - 1}{e^{-\beta\mathbf{d}_- E} - 1}\right) = \\ &= \frac{(\mathbf{d}_+ - \mathbf{d}_-)E}{4\pi\gamma\mathbf{v}} + \frac{1}{4\pi\beta\gamma\mathbf{v}} \ln\left(\frac{1 - e^{-\beta\mathbf{d}_+ E}}{1 - e^{-\beta\mathbf{d}_- E}}\right), \end{aligned} \quad (\text{A.10})$$

of which the first term equals $\frac{E}{2\pi}$ since $\mathbf{d}_+ - \mathbf{d}_- = 2\gamma\mathbf{v}$. By Eq. (A.5), we arrive at

$$\mathcal{R}_{\mathbf{v}}^{(\beta)}(E) = \frac{1}{4\pi\beta\gamma\mathbf{v}} \ln\left(\frac{1 - e^{-\beta\mathbf{d}_+ E}}{1 - e^{-\beta\mathbf{d}_- E}}\right)$$

for all $E \in \mathbb{R} \setminus \{0\}$, which completes the proof. As we have seen in this derivation, the expression for the transition rate $\mathcal{R}_{\mathbf{v}}^{(\beta)}$ applies to all velocities \mathbf{v} such that $0 < |\mathbf{v}| < 1$, and it holds $\mathcal{R}_{-\mathbf{v}}^{(\beta)} = \mathcal{R}_{\mathbf{v}}^{(\beta)}$, which is to be expected since the KMS state ω_β is homogeneous and isotropic and thus the (direction-independent) transition rate of the monopole detector should not depend on the direction of the linear motion.

B. Alternative derivation for (NESS- \mathbf{v})

The substitution used to obtain Eq. (3.11) requires that the integral in Eq. (3.10) can be split in two convergent integrals for the two terms in the integrand. These two integrals can be

calculated: Using spherical coordinates we see that

$$\begin{aligned}
& \int_{\mathbb{R}^3} \frac{1}{2\|\underline{p}\|} \frac{e^{ip_1\gamma\mathbf{v}s} e^{i\|\underline{p}\|\gamma s}}{e^{\beta(p_1)\|\underline{p}\|} - 1} d^3\underline{p} = \\
& = \int_0^\infty \int_0^{\pi/2} \frac{2\pi r}{2} \left(\frac{e^{i\gamma\mathbf{v}sr \cos(\theta)} e^{i\gamma sr}}{e^{\beta_L r} - 1} + \frac{e^{-i\gamma\mathbf{v}sr \cos(\theta)} e^{i\gamma sr}}{e^{\beta_R r} - 1} \right) \sin(\theta) d\theta dr = \\
& = \frac{-i\pi}{\gamma\mathbf{v}s} \int_0^\infty \frac{e^{i\gamma sr} (e^{i\gamma\mathbf{v}sr} - 1)}{e^{\beta_L r} - 1} dr + \frac{i\pi}{\gamma\mathbf{v}s} \int_0^\infty \frac{e^{i\gamma sr} (e^{-i\gamma\mathbf{v}sr} - 1)}{e^{\beta_R r} - 1} dr = \\
& = \frac{-i\pi}{\gamma\mathbf{v}\beta_L s} \left[\psi\left(1 - \frac{i\gamma s}{\beta_L}\right) - \psi\left(1 - \frac{i\mathbf{d}_+ s}{\beta_L}\right) \right] + \frac{i\pi}{\gamma\mathbf{v}\beta_R s} \left[\psi\left(1 - \frac{i\gamma s}{\beta_R}\right) - \psi\left(1 - \frac{i\mathbf{d}_- s}{\beta_R}\right) \right],
\end{aligned}$$

where ψ is the digamma function (logarithmic derivative of the gamma function). Here we used $\int_0^\infty \frac{e^{iax} - e^{ibx}}{e^x - 1} dx = \psi(1 - ib) - \psi(1 - ia)$ for $a, b \in \mathbb{R}$, which follows from the integral representation $\psi(z) = \int_0^\infty \left(\frac{e^{-x}}{x} - \frac{e^{-(z-1)x}}{e^x - 1} \right) dx$ for $z \in \mathbb{C}$, $\text{Re}(z) > 0$ [DLMF, 5.9.12]. Similarly,

$$\begin{aligned}
& \int_{\mathbb{R}^3} \frac{1}{2\|\underline{p}\|} \frac{e^{ip_1\gamma\mathbf{v}s} e^{-i\|\underline{p}\|\gamma s}}{e^{\beta(-p_1)\|\underline{p}\|} - 1} d^3\underline{p} = \\
& = \frac{-i\pi}{\gamma\mathbf{v}\beta_R s} \left[\psi\left(1 + \frac{i\gamma s}{\beta_R}\right) - \psi\left(1 + \frac{i\mathbf{d}_- s}{\beta_R}\right) \right] + \frac{i\pi}{\gamma\mathbf{v}\beta_L s} \left[\psi\left(1 + \frac{i\gamma s}{\beta_L}\right) - \psi\left(1 + \frac{i\mathbf{d}_+ s}{\beta_L}\right) \right].
\end{aligned}$$

Inserting these results into Eq. (3.10) and using $\psi(1 + ia) - \psi(1 - ia) = i\pi \coth(\pi a) - \frac{i}{a}$ for $a \in \mathbb{R} \setminus \{0\}$ [DLMF, 5.5.2 & 5.5.4], one finds that the imaginary parts cancel each other, resulting in Eq. (3.14).

C. Comments on effective temperatures

Consider an inertial observer moving with constant velocity $\mathbf{v} \in (-1, 1)$ relative to a heat bath of temperature $\beta^{-1} > 0$. The anisotropic radiation energy spectrum observed in some fixed direction forming an angle θ to the direction of motion has been found, e.g., in [PW68, BC68, HFSP68] in the context of the cosmic microwave background radiation as observed on Earth, and is given by $f(E, T') := E / (2\pi(e^{E/T'(\beta, \mathbf{v}, \theta)} - 1))$ with the *directional temperature* (see also [LM96, LM04])

$$T'(\beta, \mathbf{v}, \theta) = \frac{\sqrt{1 - \mathbf{v}^2}}{\beta(1 - \mathbf{v} \cos(\theta))}.$$

Looking in the direction of motion ($\theta = 0$) this equals the Doppler shifted temperature $T'(\beta, \mathbf{v}, 0) = \beta^{-1} \sqrt{(1 + \mathbf{v})/(1 - \mathbf{v})}$. A critical assessment and derivation of T' can be found in [Nak09]. Averaging $f(E, T')$ over solid angles results in the distribution given in Eq. (3.4) that appears as the transition rate of an Unruh-DeWitt detector carried by the observer and coupled to the heat bath [CM95b, LM96]. The solid angle average of T' is (see [LM96, Eq.

(8)]

$$\frac{1}{4\pi} \int_0^{2\pi} \int_0^\pi T'(\beta, \mathbf{v}, \theta) \sin(\theta) d\theta d\varphi = \frac{\sqrt{1-\mathbf{v}^2}}{2\beta} \int_0^\pi \frac{\sin(\theta)}{1-\mathbf{v}\cos(\theta)} d\theta = \frac{\sqrt{1-\mathbf{v}^2}}{2\beta\mathbf{v}} \ln\left(\frac{1+\mathbf{v}}{1-\mathbf{v}}\right),$$

where the θ -integral is solved by substituting for $1-\mathbf{v}\cos(\theta)$. This equals the lowest order of the detailed balance effective temperature in the case **(KMS- \mathbf{v})** (see Eq. (4.1)).

D. The NESS stress-energy tensor

We show that the expectation value of the stress-energy tensor in the NESS ω_N of the four-dimensional massless scalar field (Section 2.3) has block diagonal form and calculate its components. The results have been presented before in [DLSB15] for free scalar fields in $(1+d)$ -dimensional Minkowski spacetime ($d \geq 1$) and with arbitrary field mass. Here, we rederive them using the two-point function of the NESS based on [HV18].

Lemma D.1

For every $x \in \mathbb{M}$ and $\mu, \nu \in \{0, 1, 2, 3\}$ it holds

$$\omega_N(T_{\mu\nu}(x)) = \frac{1}{(2\pi)^3} \int_{\mathbb{R}^3} \frac{1}{2\|\underline{p}\|} \frac{2p_\mu p_\nu}{e^{\beta(p_1)\|\underline{p}\|} - 1} d^3\underline{p} =: \omega_N(T_{\mu\nu}), \quad (\text{D.1})$$

where $p_0 := \|\underline{p}\| \equiv (\sum_{i=1}^3 p_i^2)^{1/2}$. In 4×4 matrix form,

$$(\omega_N(T_{\mu\nu})) = \begin{pmatrix} \tilde{\mathcal{T}} & \mathbf{0}_2 \\ \mathbf{0}_2 & \text{diag}(\mathcal{T}_\perp, \mathcal{T}_\perp) \end{pmatrix}, \quad (\text{D.2})$$

where $\mathbf{0}_2$ is the 2×2 zero matrix, $\tilde{\mathcal{T}}$ is a symmetric, non-zero 2×2 matrix, and $\mathcal{T}_\perp := \omega_N(T_{22})$.

Proof.

From the definition of the stress-energy tensor (Eq. (5.1)) it follows that

$$\omega_N(T_{\mu\nu}(x)) = \left[\left(\partial_\mu \otimes \partial_\nu - \frac{1}{2} \eta_{\mu\nu} \partial_\rho \otimes \partial^\rho \right) \widetilde{W}_N \right] (x, x),$$

where Einstein's summation convention is implied, and $\widetilde{W}_N := W_N - W_{\text{vac}}$ is given by Eq. (2.10); recall that \widetilde{W}_N is a smooth function on $\mathbb{M} \times \mathbb{M}$ [HV18]. Since $\partial_0 \otimes \partial_0 e^{\pm i\|\underline{p}\|(x^0-y^0)}|_{x=y} = \|\underline{p}\|^2$ and $\partial_i \otimes \partial_j e^{i\underline{p}\cdot(x-y)}|_{x=y} = p_i p_j$ (for $i, j \in \{1, 2, 3\}$) we get, using Eq. (2.10),

$$\begin{aligned} \left(\partial_\mu \otimes \partial_\mu \widetilde{W}_N \right) (x, x) &= \frac{1}{(2\pi)^3} \int_{\mathbb{R}^3} \frac{1}{2\|\underline{p}\|} p_\mu^2 \left(\frac{1}{e^{\beta(p_1)\|\underline{p}\|} - 1} + \frac{1}{e^{\beta(-p_1)\|\underline{p}\|} - 1} \right) d^3\underline{p} = \\ &= \frac{1}{(2\pi)^3} \int_{\mathbb{R}^3} \frac{1}{2\|\underline{p}\|} \frac{2p_\mu^2}{e^{\beta(p_1)\|\underline{p}\|} - 1} d^3\underline{p} \end{aligned}$$

for $\mu \in \{0, 1, 2, 3\}$, where in the last step a substitution $-p_1 \mapsto p_1$ is performed for the second term. This implies

$$\omega_N(T_{00}(x)) = \frac{1}{2} \left[\left(\partial_0 \otimes \partial_0 + \sum_{i=1}^3 \partial_i \otimes \partial_i \right) \widetilde{W}_N \right] (x, x) = \frac{1}{(2\pi)^3} \int_{\mathbb{R}^3} \frac{1}{2\|\underline{p}\|} \frac{2p_0^2}{e^{\beta(p_1)\|\underline{p}\|} - 1} d^3\underline{p}$$

and, for $i \in \{1, 2, 3\}$,

$$\begin{aligned} \omega_N(T_{ii}(x)) &= \frac{1}{2} \left[\left(\partial_i \otimes \partial_i + \partial_0 \otimes \partial_0 - \sum_{j \neq i} \partial_j \otimes \partial_j \right) \widetilde{W}_N \right] (x, x) = \\ &= \frac{1}{2} \frac{1}{(2\pi)^3} \int_{\mathbb{R}^3} \frac{1}{2\|\underline{p}\|} \frac{2p_i^2 + 2p_0^2 - 2 \sum_{j \neq i} p_j^2}{e^{\beta(p_1)\|\underline{p}\|} - 1} d^3\underline{p} = \frac{1}{(2\pi)^3} \int_{\mathbb{R}^3} \frac{1}{2\|\underline{p}\|} \frac{2p_i^2}{e^{\beta(p_1)\|\underline{p}\|} - 1} d^3\underline{p}. \end{aligned}$$

Furthermore, since $\partial_0 \otimes \partial_i e^{i\underline{p} \cdot (\underline{x} - \underline{y})} e^{\pm i\|\underline{p}\|(x^0 - y^0)} \Big|_{x=y} = \pm \|\underline{p}\| p_i \equiv \pm p_0 p_i$ (for $i \in \{1, 2, 3\}$),

$$\begin{aligned} \omega_N(T_{i0}(x)) &= \omega_N(T_{0i}(x)) = \left(\partial_0 \otimes \partial_i \widetilde{W}_N \right) (x, x) = \\ &= \frac{1}{(2\pi)^3} \int_{\mathbb{R}^3} \frac{1}{2\|\underline{p}\|} p_0 p_i \left(\frac{1}{e^{\beta(p_1)\|\underline{p}\|} - 1} - \frac{1}{e^{\beta(-p_1)\|\underline{p}\|} - 1} \right) d^3\underline{p} = \\ &= \delta_{i,1} \frac{1}{(2\pi)^3} \int_{\mathbb{R}^3} \frac{1}{2\|\underline{p}\|} \frac{2p_0 p_i}{e^{\beta(p_1)\|\underline{p}\|} - 1} d^3\underline{p}, \end{aligned}$$

where the last step again follows from substituting $-p_1 \mapsto p_1$ in the second term, which cancels the remaining term unless $i = 1$. Likewise, one observes that

$$\begin{aligned} \omega_N(T_{i1}(x)) &= \omega_N(T_{1i}(x)) = \left(\partial_1 \otimes \partial_i \widetilde{W}_N \right) (x, x) = \\ &= \frac{1}{(2\pi)^3} \int_{\mathbb{R}^3} \frac{1}{2\|\underline{p}\|} p_1 p_i \left(\frac{1}{e^{\beta(p_1)\|\underline{p}\|} - 1} + \frac{1}{e^{\beta(-p_1)\|\underline{p}\|} - 1} \right) d^3\underline{p} = 0 \end{aligned}$$

for $i \in \{2, 3\}$. Finally,

$$\omega_N(T_{32}(x)) = \omega_N(T_{23}(x)) = \left(\partial_2 \otimes \partial_3 \widetilde{W}_N \right) (x, x) = \frac{1}{(2\pi)^3} \int_{\mathbb{R}^3} \frac{1}{2\|\underline{p}\|} \frac{2p_2 p_3}{e^{\beta(p_1)\|\underline{p}\|} - 1} d^3\underline{p} = 0$$

as the integrand is odd in p_2 and p_3 . Hence Eq. (D.1) is proven. Due to the independence from $x \in \mathbb{M}$ we can omit it in the notation. The block diagonal form in Eq. (D.2) follows from the above calculations and $\omega_N(T_{22}) = \omega_N(T_{33})$. \square

Eq. (D.1) coincides with the expected stress-energy tensor for the NESS considered in [DLSB15], and one can determine the (00) and (01) components from the general expressions

in [DLSB15, Appendix A]. For completeness, we present the calculation of the non-zero components in our case of a four-dimensional massless scalar field, and thereby derive the value of $\kappa(\beta_L, \beta_R)$ that appears in Proposition 5.1.

Lemma D.2

The non-zero components of the expected stress-energy tensor $\mathcal{T}_{\mu\nu} := \omega_N(T_{\mu\nu})$ for the NESS ω_N (Eq. (D.1)) are given by

$$\mathcal{T}_{00} = \frac{\pi^2}{60} \left(\frac{1}{\beta_L^4} + \frac{1}{\beta_R^4} \right), \quad \mathcal{T}_{01} = \frac{\pi^2}{120} \left(\frac{1}{\beta_L^4} - \frac{1}{\beta_R^4} \right), \quad \mathcal{T}_{ii} = \frac{1}{3} \mathcal{T}_{00}$$

for $i \in \{1, 2, 3\}$, and thus, if $\beta_L \neq \beta_R$,

$$\frac{\mathcal{T}_{00} + \mathcal{T}_{11}}{2\mathcal{T}_{01}} \equiv \frac{2\mathcal{T}_{00}}{3\mathcal{T}_{01}} = \frac{4}{3} \frac{\beta_R^4 + \beta_L^4}{\beta_R^4 - \beta_L^4}.$$

Proof.

By [EMOT54, Sec. 6.3, (7)],

$$\int_0^\infty \frac{r^3}{e^{\beta r} - 1} dr = \frac{1}{\beta^4} \Gamma(4) \zeta(4) = \frac{\pi^4}{15\beta^4}, \quad \beta > 0$$

for the Riemann zeta function ζ and gamma function Γ . Therefore,

$$\begin{aligned} \mathcal{T}_{00} &= \frac{1}{(2\pi)^3} \int_{\mathbb{R}^3} \frac{\|\underline{p}\|}{e^{\beta(p_1)\|\underline{p}\|} - 1} d^3\underline{p} = \\ &= \frac{1}{(2\pi)^3} \int_{\{p_1 > 0\} \times \mathbb{R}^2} \frac{\|\underline{p}\|}{e^{\beta_L \|\underline{p}\|} - 1} d^3\underline{p} + \frac{1}{(2\pi)^3} \int_{\{p_1 < 0\} \times \mathbb{R}^2} \frac{\|\underline{p}\|}{e^{\beta_R \|\underline{p}\|} - 1} d^3\underline{p} = \\ &= \frac{1}{(2\pi)^3} 2\pi \int_0^\infty \frac{r}{e^{\beta_L r} - 1} r^2 dr + \frac{1}{(2\pi)^3} 2\pi \int_0^\infty \frac{r}{e^{\beta_R r} - 1} r^2 dr = \frac{\pi^2}{60} \left(\frac{1}{\beta_L^4} + \frac{1}{\beta_R^4} \right), \end{aligned}$$

where the integral over p_1 is split following the definition of $\beta(p_1)$ (Eq. (2.9)) and the resulting integrals are calculated in spherical coordinates on $(0, \infty) \times \mathbb{R}^2$, where integrals over the angular coordinates equal 2π . In the same way, we get

$$\begin{aligned} \mathcal{T}_{01} &= \frac{1}{(2\pi)^3} \int_{\mathbb{R}^3} \frac{p_1}{e^{\beta(p_1)\|\underline{p}\|} - 1} d^3\underline{p} = \frac{1}{(2\pi)^3} \int_{\{p_1 > 0\} \times \mathbb{R}^2} p_1 \left(\frac{1}{e^{\beta_L \|\underline{p}\|} - 1} - \frac{1}{e^{\beta_R \|\underline{p}\|} - 1} \right) d^3\underline{p} = \\ &= \frac{1}{(2\pi)^3} \pi \int_0^\infty r^3 \left(\frac{1}{e^{\beta_L r} - 1} - \frac{1}{e^{\beta_R r} - 1} \right) dr = \frac{\pi^2}{120} \left(\frac{1}{\beta_L^4} - \frac{1}{\beta_R^4} \right). \end{aligned}$$

Finally,

$$\mathcal{T}_{ii} = \frac{1}{(2\pi)^3} \int_{\mathbb{R}^3} \frac{1}{\|\underline{p}\|} \frac{p_i^2}{e^{\beta(p_1)\|\underline{p}\|} - 1} d^3\underline{p} = \frac{1}{(2\pi)^3} \int_{\{p_1 > 0\} \times \mathbb{R}^2} \frac{p_i^2}{\|\underline{p}\|} \left(\frac{1}{e^{\beta_L \|\underline{p}\|} - 1} + \frac{1}{e^{\beta_R \|\underline{p}\|} - 1} \right) d^3\underline{p} =$$

$$= \frac{1}{(2\pi)^3} \frac{2\pi}{3} \int_0^\infty r^3 \left(\frac{1}{e^{\beta_L r} - 1} + \frac{1}{e^{\beta_R r} - 1} \right) dr = \frac{\pi^2}{180} \left(\frac{1}{\beta_L^4} + \frac{1}{\beta_R^4} \right) \equiv \frac{1}{3} \mathcal{T}_{00}$$

for $i \in \{1, 2, 3\}$, which reflects the tracelessness of the stress-energy tensor.

□

References

- [Abo07] W. K. ABOU SALEM, On the Quasi-Static Evolution of Nonequilibrium Steady States, *Annales Henri Poincaré* **8** (2007), 569–596. <https://doi.org/10.1007/s00023-006-0316-2>.
- [AP03] W. H. ASCHBACHER and C.-A. PILLET, Non-equilibrium steady states of the XY chain, *Journal of Statistical Physics* **112** (2003), 1153–1175. <https://doi.org/10.1023/a:1024619726273>.
- [BD12] D. BERNARD and B. DOYON, Energy flow in non-equilibrium conformal field theory, *Journal of Physics A: Mathematical and Theoretical* **45** (2012), 362001. <https://doi.org/10.1088/1751-8113/45/36/362001>.
- [BD15] D. BERNARD and B. DOYON, Non-Equilibrium Steady States in Conformal Field Theory, *Annales Henri Poincaré* **16** (2015), 113–161. <https://doi.org/10.1007/s00023-014-0314-8>.
- [BDLS15] M. J. BHASEEN, B. DOYON, A. LUCAS, and K. SCHALM, Energy flow in quantum critical systems far from equilibrium, *Nature Physics* **11** (2015), 509–514. <https://doi.org/10.1038/nphys3320>.
- [BEG⁺20] S. BIERMANN, S. ERNE, C. GOODING, J. LOUKO, J. SCHMIEDMAYER, W. G. UNRUH, and S. WEINFURTNER, Unruh and analogue Unruh temperatures for circular motion in $3 + 1$ and $2 + 1$ dimensions, *Physical Review D* **102** (2020), 085006. <https://doi.org/10.1103/physrevd.102.085006>.
- [BD82] N. D. BIRRELL and P. C. W. DAVIES, *Quantum Fields in Curved Space*, Cambridge University Press, 1982. <https://doi.org/10.1017/cbo9780511622632>.
- [BC68] R. N. BRACEWELL and E. K. CONKLIN, An observer moving in the 3° K radiation field, *Nature* **219** (1968), 1343–1344. <https://doi.org/10.1038/2191343a0>.
- [BR97] O. BRATTELI and D. W. ROBINSON, *Operator Algebras and Quantum Statistical Mechanics 2*, 2nd ed., Springer Berlin Heidelberg, 1997. <https://doi.org/10.1007/978-3-662-03444-6>.
- [BOR02] D. BUCHHOLZ, I. OJIMA, and H. ROOS, Thermodynamic Properties of Non-equilibrium States in Quantum Field Theory, *Annals of Physics* **297** (2002), 219–242. <https://doi.org/10.1006/aphy.2002.6222>.
- [BS13] D. BUCHHOLZ and C. SOLVEEN, Unruh effect and the concept of temperature, *Classical and Quantum Gravity* **30** (2013), 085011. <https://doi.org/10.1088/0264-9381/30/8/085011>.
- [BL23] C. R. D. BUNNEY and J. LOUKO, Circular motion analogue Unruh effect in a $2 + 1$ thermal bath: robbing from the rich and giving to the poor, *Classical and Quantum Gravity* **40** (2023), 155001. <https://doi.org/10.1088/1361-6382/acde3b>.
- [BPPL24] C. R. D. BUNNEY, L. PARRY, T. R. PERCHE, and J. LOUKO, Ambient temperature versus ambient acceleration in the circular motion Unruh effect, *Physical Review D* **109** (2024), 065001. <https://doi.org/10.1103/physrevd.109.065001>.
- [CH71] H. CALLEN and G. HORWITZ, Relativistic Thermodynamics, *American Journal of Physics* **39** (1971), 938–947. <https://doi.org/10.1119/1.1986330>.
- [CJ03] J. CASAS-VÁZQUEZ and D. JOU, Temperature in non-equilibrium states: a review of open problems and current proposals, *Reports on Progress in Physics* **66** (2003), 1937–2023. <https://doi.org/10.1088/0034-4885/66/11/r03>.

- [CS69] G. CAVALLERI and G. SALGARELLI, Revision of the relativistic dynamics with variable rest mass and application to relativistic thermodynamics, *Il Nuovo Cimento A* **62** (1969), 722–754. <https://doi.org/10.1007/bf02819595>.
- [Cos04] S. S. COSTA, Some properties of a thermal bath as seen by an uniformly moving observer, *Physics Letters A* **328** (2004), 270–273. <https://doi.org/10.1016/j.physleta.2004.06.041>.
- [CM95a] S. S. COSTA and G. E. A. MATSAS, Background thermal contributions in testing the Unruh effect, *Physical Review D* **52** (1995), 3466–3471. <https://doi.org/10.1103/physrevd.52.3466>.
- [CM95b] S. S. COSTA and G. E. A. MATSAS, Temperature and relativity, *Physics Letters A* **209** (1995), 155–159. [https://doi.org/10.1016/0375-9601\(95\)00843-7](https://doi.org/10.1016/0375-9601(95)00843-7).
- [CHM08] L. C. B. CRISPINO, A. HIGUCHI, and G. E. A. MATSAS, The Unruh effect and its applications, *Reviews of Modern Physics* **80** (2008), 787–838. <https://doi.org/10.1103/revmodphys.80.787>.
- [DeW79] B. S. DEWITT, Quantum gravity: the new synthesis, in *General Relativity: An Einstein Centenary Survey* (S. W. HAWKING and W. ISRAEL, eds.), Cambridge University Press, 1979, pp. 680–745.
- [DLMF] NIST Digital Library of Mathematical Functions, <http://dlmf.nist.gov>, Release 1.2.4 of 2025-03-15, F. W. J. Olver, A. B. Olde Daalhuis, D. W. Lozier, B. I. Schneider, R. F. Boisvert, C. W. Clark, B. R. Miller, B. V. Saunders, H. S. Cohl, and M. A. McClain, eds.
- [DLSB15] B. DOYON, A. LUCAS, K. SCHALM, and M. J. BHASEEN, Non-equilibrium steady states in the Klein-Gordon theory, *Journal of Physics A: Mathematical and Theoretical* **48** (2015), 095002. <https://doi.org/10.1088/1751-8113/48/9/095002>.
- [EMOT54] A. ERDÉLYI, W. MAGNUS, F. OBERHETTINGER, and F. G. TRICOMI (eds.), *Tables of Integral Transforms, Volume I, Bateman Manuscript Project, California Institute of Technology*, McGraw-Hill Book Company, Inc., 1954.
- [FPM17] C. FARIÁS, V. A. PINTO, and P. S. MOYA, What is the temperature of a moving body?, *Scientific Reports* **7** (2017), 17657. <https://doi.org/10.1038/s41598-017-17526-4>.
- [FJL16] C. J. FEWSTER, B. A. JUÁREZ-AUBRY, and J. LOUKO, Waiting for Unruh, *Classical and Quantum Gravity* **33** (2016), 165003. <https://doi.org/10.1088/0264-9381/33/16/165003>.
- [FR20] C. J. FEWSTER and K. REJZNER, Algebraic Quantum Field Theory – An Introduction, in *Progress and Visions in Quantum Theory in View of Gravity* (F. FINSTER, D. GIULINI, J. KLEINER, and J. TOLKSDORF, eds.), Birkhäuser Basel, 2020, pp. 1–61. https://doi.org/10.1007/978-3-030-38941-3_1.
- [FV03] C. J. FEWSTER and R. VERCH, Stability of Quantum Systems at Three Scales: Passivity, Quantum Weak Energy Inequalities and the Microlocal Spectrum Condition, *Communications in Mathematical Physics* **240** (2003), 329–375. <https://doi.org/10.1007/s00220-003-0884-7>.
- [FV15] C. J. FEWSTER and R. VERCH, Algebraic Quantum Field Theory in Curved Spacetimes, in *Advances in Algebraic Quantum Field Theory* (R. BRUNETTI, C. DAPPIAGGI, K. FREDENHAGEN, and J. YNGVASON, eds.), Springer International Publishing, 2015, pp. 125–189. https://doi.org/10.1007/978-3-319-21353-8_4.
- [FZ11] V. P. FROLOV and A. ZELNIKOV, *Introduction to Black Hole Physics*, Oxford University Press, 2011. <https://doi.org/10.1093/acprof:oso/9780199692293.001.0001>.
- [GJMT20] M. GOOD, B. A. JUÁREZ-AUBRY, D. MOUSTOS, and M. TEMIRKHAN, Unruh-like effects: effective temperatures along stationary worldlines, *Journal of High Energy Physics* **2020** (2020), 59. [https://doi.org/10.1007/jhep06\(2020\)059](https://doi.org/10.1007/jhep06(2020)059).
- [HHW67] R. HAAG, N. M. HUGENHOLTZ, and M. WINNINK, On the equilibrium states in quantum statistical mechanics, *Communications in Mathematical Physics* **5** (1967), 215–236. <https://doi.org/10.1007/bf01646342>.
- [Haa96] R. HAAG, *Local Quantum Physics*, 2nd ed., Springer Berlin Heidelberg, 1996. <https://doi.org/10.1007/978-3-642-61458-3>.
- [HV18] T.-P. HACK and R. VERCH, Non-equilibrium steady states for the interacting Klein-Gordon field in 1+3 dimensions, 2018. <https://doi.org/10.48550/ARXIV.1806.00504>.

- [HFSP68] G. R. HENRY, R. B. FEDUNIAK, J. E. SILVER, and M. A. PETERSON, Distribution of Blackbody Cavity Radiation in a Moving Frame of Reference, *Physical Review* **176** (1968), 1451–1455. <https://doi.org/10.1103/physrev.176.1451>.
- [Hin83] K. J. HINTON, Particle detectors in Rindler and Schwarzschild space-times, *Journal of Physics A: Mathematical and General* **16** (1983), 1937–1946. <https://doi.org/10.1088/0305-4470/16/9/018>.
- [HL18] S. HOLLANDS and R. LONGO, Non-equilibrium Thermodynamics and Conformal Field Theory, *Communications in Mathematical Physics* **357** (2018), 43–60. <https://doi.org/10.1007/s00220-017-2938-2>.
- [HD15] M. HOOGEVEEN and B. DOYON, Entanglement negativity and entropy in non-equilibrium conformal field theory, *Nuclear Physics B* **898** (2015), 78–112. <https://doi.org/10.1016/j.nuclphysb.2015.06.021>.
- [HN20] H. HOSHINO and S. NAKAMURA, Proper effective temperature of nonequilibrium steady state, *Progress of Theoretical and Experimental Physics* **2020** (2020), 093B09. <https://doi.org/10.1093/ptep/ptaa110>.
- [JP02a] V. JAKŠIĆ and C.-A. PILLET, Mathematical Theory of Non-Equilibrium Quantum Statistical Mechanics, *Journal of Statistical Physics* **108** (2002), 787–829. <https://doi.org/10.1023/a:1019818909696>.
- [JP02b] V. JAKŠIĆ and C.-A. PILLET, Non-Equilibrium Steady States of Finite Quantum Systems Coupled to Thermal Reservoirs, *Communications in Mathematical Physics* **226** (2002), 131–162. <https://doi.org/10.1007/s002200200602>.
- [JM19] B. A. JUÁREZ-AUBRY and D. MOUSTOS, Asymptotic states for stationary Unruh-DeWitt detectors, *Physical Review D* **100** (2019), 025018. <https://doi.org/10.1103/physrevd.100.025018>.
- [KW91] B. S. KAY and R. M. WALD, Theorems on the uniqueness and thermal properties of stationary, nonsingular, quasifree states on spacetimes with a bifurcate Killing horizon, *Physics Reports* **207** (1991), 49–136. [https://doi.org/10.1016/0370-1573\(91\)90015-E](https://doi.org/10.1016/0370-1573(91)90015-E).
- [KM15] I. KHAVKINE and V. MORETTI, Algebraic QFT in Curved Spacetime and Quasifree Hadamard States: An Introduction, in *Advances in Algebraic Quantum Field Theory* (R. BRUNETTI, C. DAPPIAGGI, K. FREDENHAGEN, and J. YNGVASON, eds.), Springer International Publishing, 2015, pp. 191–251. https://doi.org/10.1007/978-3-319-21353-8_5.
- [Kub57] R. KUBO, Statistical-mechanical theory of irreversible processes I. General theory and simple applications to magnetic and conduction problems, *Journal of the Physical Society of Japan* **12** (1957), 570–586. <https://doi.org/10.1143/jpsj.12.570>.
- [LM04] P. T. LANDSBERG and G. E. A. MATSAS, The impossibility of a universal relativistic temperature transformation, *Physica A: Statistical Mechanics and its Applications* **340** (2004), 92–94. <https://doi.org/10.1016/j.physa.2004.03.081>.
- [LM96] P. T. LANDSBERG and G. E. A. MATSAS, Laying the ghost of the relativistic temperature transformation, *Physics Letters A* **223** (1996), 401–403. [https://doi.org/10.1016/s0375-9601\(96\)00791-8](https://doi.org/10.1016/s0375-9601(96)00791-8).
- [LS06] J. LOUKO and A. SATZ, How often does the Unruh-DeWitt detector click? Regularization by a spatial profile, *Classical and Quantum Gravity* **23** (2006), 6321–6343. <https://doi.org/10.1088/0264-9381/23/22/015>.
- [LS08] J. LOUKO and A. SATZ, Transition rate of the Unruh-DeWitt detector in curved spacetime, *Classical and Quantum Gravity* **25** (2008), 055012. <https://doi.org/10.1088/0264-9381/25/5/055012>.
- [MS59] P. C. MARTIN and J. SCHWINGER, Theory of many-particle systems. I, *Physical Review* **115** (1959), 1342–1373. <https://doi.org/10.1103/physrev.115.1342>.
- [MA98] K.-P. MARZLIN and J. AUDRETSCH, States insensitive to the Unruh effect in multilevel detectors, *Physical Review D* **57** (1998), 1045–1051. <https://doi.org/10.1103/physrevd.57.1045>.

- [MMS07a] M. MERKLI, M. MÜCK, and I. M. SIGAL, Instability of equilibrium states for coupled heat reservoirs at different temperatures, *Journal of Functional Analysis* **243** (2007), 87–120. <https://doi.org/10.1016/j.jfa.2006.10.017>.
- [MMS07b] M. MERKLI, M. MÜCK, and I. M. SIGAL, Theory of Non-Equilibrium Stationary States as a Theory of Resonances, *Annales Henri Poincaré* **8** (2007), 1539–1593. <https://doi.org/10.1007/s00023-007-0346-4>.
- [Mou18] D. MOUSTOS, Asymptotic states of accelerated detectors and universality of the Unruh effect, *Physical Review D* **98** (2018), 065006. <https://doi.org/10.1103/physrevd.98.065006>.
- [Nak09] T. K. NAKAMURA, Lorentz transform of black-body radiation temperature, *Europhysics Letters* **88** (2009), 20004. <https://doi.org/10.1209/0295-5075/88/20004>.
- [Neu80] G. NEUGEBAUER, *Relativistische Thermodynamik*, De Gruyter, 1980. <https://doi.org/10.1515/9783112621721>.
- [Obe90] F. OBERHETTINGER, *Tables of Fourier Transforms and Fourier Transforms of Distributions*, Springer Berlin Heidelberg, 1990. <https://doi.org/10.1007/978-3-642-74349-8>.
- [Oga04] Y. OGATA, The Stability of the Non-Equilibrium Steady States, *Communications in Mathematical Physics* **245** (2004), 577–609. <https://doi.org/10.1007/s00220-003-1011-5>.
- [PS87] T. PADMANABHAN and T. P. SINGH, Response of an accelerated detector coupled to the stress-energy tensor, *Classical and Quantum Gravity* **4** (1987), 1397–1407. <https://doi.org/10.1088/0264-9381/4/5/033>.
- [PA20] N. PAPADATOS and C. ANASTOPOULOS, Relativistic quantum thermodynamics of moving systems, *Physical Review D* **102** (2020), 085005. <https://doi.org/10.1103/physrevd.102.085005>.
- [PL25] L. J. A. PARRY and J. LOUKO, Connecting the circular and drifted Rindler Unruh effects, *Physical Review D* **111** (2025), 025012. <https://doi.org/10.1103/physrevd.111.025012>.
- [PV25] A. G. PASSEGGER and R. VERCH, Disjointness of inertial KMS states and the role of Lorentz symmetry in thermalization, *Reviews in Mathematical Physics* **37** (2025), 2430009. <https://doi.org/10.1142/S0129055X24300097>.
- [PW68] P. J. E. PEEBLES and D. T. WILKINSON, Comment on the Anisotropy of the Primeval Fireball, *Physical Review* **174** (1968), 2168. <https://doi.org/10.1103/physrev.174.2168>.
- [PW78] W. PUSZ and S. L. WORONOWICZ, Passive states and KMS states for general quantum systems, *Communications in Mathematical Physics* **58** (1978), 273–290. <https://doi.org/10.1007/bf01614224>.
- [Rad96] M. J. RADZIKOWSKI, Micro-local approach to the Hadamard condition in quantum field theory on curved space-time, *Communications in Mathematical Physics* **179** (1996), 529–553. <https://doi.org/10.1007/bf02100096>.
- [Rin77] W. RINDLER, *Essential Relativity*, 2nd ed., Springer Berlin Heidelberg, 1977. <https://doi.org/10.1007/978-3-642-86650-0>.
- [Rue00] D. RUELLE, Natural Nonequilibrium States in Quantum Statistical Mechanics, *Journal of Statistical Physics* **98** (2000), 57–75. <https://doi.org/10.1023/a:1018618704438>.
- [Rue01] D. RUELLE, Entropy Production in Quantum Spin Systems, *Communications in Mathematical Physics* **224** (2001), 3–16. <https://doi.org/10.1007/s002200100534>.
- [Rue02] D. RUELLE, How should one define entropy production for nonequilibrium quantum spin systems?, *Reviews in Mathematical Physics* **14** (2002), 701–707. <https://doi.org/10.1142/s0129055x02001296>.
- [SV00] H. SAHLMANN and R. VERCH, Passivity and Microlocal Spectrum Condition, *Communications in Mathematical Physics* **214** (2000), 705–731. <https://doi.org/10.1007/s002200000297>.
- [Sat07] A. SATZ, Then again, how often does the Unruh-DeWitt detector click if we switch it carefully?, *Classical and Quantum Gravity* **24** (2007), 1719–1731. <https://doi.org/10.1088/0264-9381/24/7/003>.

- [Sch04] S. SCHLICHT, Considerations on the Unruh effect: causality and regularization, *Classical and Quantum Gravity* **21** (2004), 4647–4660. <https://doi.org/10.1088/0264-9381/21/19/011>.
- [Sch09] B. SCHUTZ, *A First Course in General Relativity*, 2nd ed., Cambridge University Press, 2009. <https://doi.org/10.1017/cbo9780511984181>.
- [Sew08] G. L. SEWELL, On the question of temperature transformations under Lorentz and Galilei boosts, *Journal of Physics A: Mathematical and Theoretical* **41** (2008), 382003. <https://doi.org/10.1088/1751-8113/41/38/382003>.
- [Sew09] G. L. SEWELL, Statistical thermodynamics of moving bodies, *Reports on Mathematical Physics* **64** (2009), 285–291. [https://doi.org/10.1016/s0034-4877\(09\)90033-7](https://doi.org/10.1016/s0034-4877(09)90033-7).
- [Sew10] G. L. SEWELL, Note on the relativistic thermodynamics of moving bodies, *Journal of Physics A: Mathematical and Theoretical* **43** (2010), 485001. <https://doi.org/10.1088/1751-8113/43/48/485001>.
- [SL77] H. SPOHN and J. L. LEBOWITZ, Stationary non-equilibrium states of infinite harmonic systems, *Communications in Mathematical Physics* **54** (1977), 97–120. <https://doi.org/10.1007/bf01614132>.
- [Tak86] S. TAKAGI, Vacuum Noise and Stress Induced by Uniform Acceleration: Hawking-Unruh Effect in Rindler Manifold of Arbitrary Dimension, *Progress of Theoretical Physics Supplement* **88** (1986), 1–142. <https://doi.org/10.1143/PTP.88.1>.
- [Tas01] S. TASAKI, Nonequilibrium stationary states of noninteracting electrons in a one-dimensional lattice, *Chaos, Solitons & Fractals* **12** (2001), 2657–2674. [https://doi.org/10.1016/s0960-0779\(01\)00080-7](https://doi.org/10.1016/s0960-0779(01)00080-7).
- [Unr76] W. G. UNRUH, Notes on black-hole evaporation, *Physical Review D* **14** (1976), 870–892. <https://doi.org/10.1103/physrevd.14.870>.
- [UW84] W. G. UNRUH and R. M. WALD, What happens when an accelerating observer detects a Rindler particle, *Physical Review D* **29** (1984), 1047–1056. <https://doi.org/10.1103/physrevd.29.1047>.
- [Wel00] H. A. WELDON, Thermal Green functions in coordinate space for massless particles of any spin, *Physical Review D* **62** (2000), 056010. <https://doi.org/10.1103/physrevd.62.056010>.